Producing a Bioplastic from Biodiesel Waste: Poly(hydroxybutyrate) using Crude Glycerol

A Technical Report submitted to the Department of Chemical Engineering

Presented to the Faculty of the School of Engineering and Applied Science

University of Virginia • Charlottesville, Virginia

In Partial Fulfillment of the Requirements for the Degree

Bachelor of Science, School of Engineering

Hamsini Muralikrishnan

Spring, 2023

Technical Project Team Members

Alexa Cuomo

Isabelle Deadman

Allison Feeney

Justine Yun

On my honor as a University Student, I have neither given nor received unauthorized aid on this assignment as defined by the Honor Guidelines for Thesis-Related Assignments

Eric W. Anderson, Department of Chemical Engineering

Table of Contents

1. Executive Summary

Overview:

In the face of massive amounts of plastic pollution in today's world, we sought to design a plant to produce a biodegradable plastic out of biodiesel waste. Our plant will have a PHB production capacity of 7.32 kilotons per annum (ktpa). We chose this scale because we plan to partner with a large biodiesel company to buy all of 29.9 ktpa of their waste glycerol from their biorefineries in Iowa.

Process Summary:

The goal of the upstream process is to provide optimal conditions to grow the maximum amount of PHB. The fermentation substrate is crude glycerol (80 wt%), a byproduct of biodiesel production. First, *C. necator* will be grown in a seed train (R-101) to provide high cell density inoculum to the large fed batch bioreactors (R-102). Then, the inoculate will be transferred to large fed-batch reactors where *C. necator* will be further grown to accumulate PHB. Over the growth phase, *C. necator* grows in the glycerol media and PHB slowly accumulates within the cells' cytoplasm with the supply of nitrogen in the form of ammonium hydroxide. Around two-thirds of the way through the fermentation process, the nitrogen source to the reactor is replaced with potassium hydroxide (KOH), which initiates "nitrogen stress response" and causes the microbes to store mass amounts of substrate (Koch et al., 2019). Then, the microbes produce mass amounts of PHB in the nitrogen depletion phase. Once the maximum concentration of PHB is achieved at 33.5 hours, the contents of the reactor is sent downstream to separate, purify, and package the PHB to be sold to plastic manufacturers. First the fermenter effluent is sent through two homogenizers to perform cell lysis. Then the disrupted cells are sent through a series of two disc-stack centrifuges to isolate the PHB. Then the PHB and water mixture is sent through a

spray dryer and the 99.2% pure PHB is then sent through a plastic extrusion process to produce 25 kg bags of 3mm plastic pellets.

Economics:

Building this PHB plant is not economically feasible. The expected revenue from selling PHB is $32.9 MM/yr. Production and fixed costs far outweigh anticipated revenue for an average cash loss of $41.2 MM/yr. The largest variable cost is raw materials at $24.6 MM/year. The largest fixed cost is the overhead expenses at $21 MM/year (Figure 12.7.1). Furthermore, a discounted cash flow analysis of the plant was performed over the expected lifetime of the plant, 20 years, at a discount rate of 15%. It was found that it only loses money over time and will never break even or turn a profit. However, if the plant was changed to produce a smaller amount of medical grade PHB sold at $27/kg, the project would break even after 7 years and after 20 years have an internal rate of return of 25%. While the concepts behind the plant are sustainable in theory, the design itself is not sustainable if it requires massive investments from federal funds or a dramatic change in market demand and value. In the 21st century, petrochemical-derived plastics are still far cheaper to produce and consume from a price standpoint. Until the human and environmental health effects of plastic are included in this cost, it is likely a large-scale bioplastic plant will continue to be infeasible.

2. Background and Motivation for a Sustainable Materials Design Project

Plastic waste is a growing global environmental concern. From 1950 to 2019, plastic waste production has grown exponentially, with 9.54 billion tons of plastic waste produced worldwide in 2019 alone (Ritchie & Roser, 2018). Despite efforts to recycle, only three million of the 35.7 million tons of generated plastic were recycled in the United States in 2018, a recycling rate of 8.7% (US EPA, 2017). Single-use plastics are abundant especially in the

pharmaceutical and food industries in the form of packaging. It is difficult to recycle biopharma waste due to components such as silicon, polyethylene and polypropylene in bioreactor bags or chemical waste containers, so the waste is generally burned or landfilled (Kohn, 2019). Considering the millions of tons of plastic that end up in landfills and oceans and can take up to hundreds of years to break down, plastic pollution poses a great threat to environmental and human health.

The unsustainable nature of plastics has motivated investment in alternatives to conventional plastics produced from petrochemicals. One such class of alternative plastics is polyhydroxyalkanoates, or PHAs, which are naturally biodegradable polyesters synthesized by microorganisms (Li et al., 2016). These sustainably produced plastics could mitigate the issue of plastic waste due to their shorter degradation timescales. While PHAs are promising, previous ventures into their production have not always been successful. For example, a joint venture between Archer Daniels Midland and Metabolix for a PHA plant in Iowa that was opened in 2010 ended up closing down only a few years later due to rising costs and market uncertainty (Tullo, 2015). Some PHAs also have disadvantages to traditionally-produced plastics in terms of their mechanical properties, which also hinders their popularity (Li et al., 2016).

Today, there is a more widespread consciousness of the importance of sustainability which can create a stronger market for plastics such as PHAs. This allows for a more serious investment in transitioning away from unsustainable plastics. In particular, polyhydroxybutyrate (PHB) is a type of PHA that has thermomechanical properties which are advantageous in certain applications compared to petroleum-based polymers (McAdam et al., 2020). Although there are currently other widely used biopolymers, namely polylactic acid (PLA), these require industrial facilities in order for them to biodegrade (*The Plastic Alternative the World Needs*, 2022). This

makes PHB a superior alternative to PLA in that it can easily biodegrade in an ambient environment in the presence of microorganisms. Essentially, this makes PHB attractive as it is both a bio-based and biodegradable polymer (Waldrop, 2021). We can create an even more sustainable process for PHB production by using a crude glycerol waste stream from a biodiesel production facility as the carbon feedstock for the microorganisms. As noted by Castillo et al. (2017), PHB has high production costs, so utilizing crude glycerol as a starting material in this process proves to be economically attractive and feasible.

3. Targeted Product: Polyhydroxybutyrate

The final product of our process will be PHB pellets of 99.9% purity that can be sold for use in other manufacturing processes. Because we are producing pellets, other manufacturers would have the option to blend the PHB with other raw materials to improve certain thermal and mechanical properties and adjust them to their specific needs (Li et al., 2016). PHB is a polymer synthesized starting from acetyl-CoA molecules that are eventually reduced to 3-hydroxybutyryl-CoA monomers (see Figure 3.1), which are connected through an ester bond when they are polymerized inside microorganisms (Koch & Forchhammer, 2021).

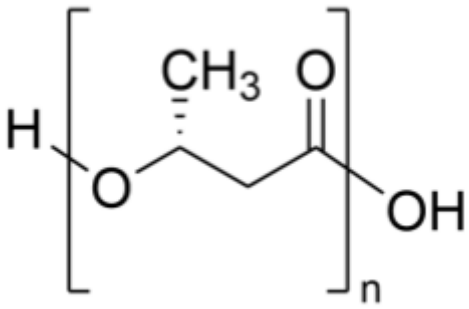

Figure 3.1. PHB Monomer (3-hydroxybutyryl) Structure

The functional properties of PHB are defined based on the microorganisms and growth conditions involved in the synthesis steps (Castillo et al., 2017). The molecular weight of the produced polymer can be altered by varying the initial carbon-nitrogen ratio in the batch culture.

Thermomechanical properties such as elasticity, tensile strength, and crystallinity, change based on polymer molecular weight. For example, at low molecular weights, PHB exhibits more rigidity, while at high molecular weights, PHB exhibits more elastic properties and high tensile strength. The flexibility of PHB's properties lends it to different functions and applications. For biomedical applications, high polymer elasticity and tensile strength are needed for devices such as surgical implants or biomaterials in tissue engineering to function efficiently. Tripathi et al. conducted a similar study named *Effect of nutritional supplements on bio-plastics (PHB) production utilizing sugar refinery waste with potential application in food packaging*, in which researchers compare the effectiveness of PHA, PHB, and polypropylene (PP) based on their physicochemical and thermomechanical properties (Dutt Tripathi et al., 2019). The degree of polymerization of the PHB (derived from cane molasses) along with observed characteristics such as high enthalpy of fusion, molecular weight, and crystallinity were noted more suitable for food packaging and biomedical applications compared to PHA and PP. The researchers found that when PHB exhibited high crystallinity, this is indicative of good flexibility and gas barrier properties, which prove integral for food packaging material and preserving freshness. PHB has superior barrier properties to popular plastics such as PP, polyethylene (PE), polyethylene terephthalate (PET), and polyvinyl chloride (PVC) as well as greater rigidity than PP (McAdam et al., 2020). It exhibits a degree of crystallinity of around 50-60% which is comparable to PP, to which PHB also has a similar melting temperature range and tensile strength (McAdam et al., 2020). PHB is considered a green alternative to polypropylene (PP) and polyethylene (PE) due to their similar properties (Table 3.1). This will lend PHB to have properties similar to PP which is a universally used plastic for a wide range of applications (McAdam et al., 2020). Similar to PP, PHB can be used for consumer single-use plastic products. However, since PHB is

biodegradable, it cannot be used in long term applications such as for industrial use. PHB has a lower melting point, elongation at break, and tensile strength than polyethylene terephthalate (PET). PHB is therefore more temperature sensitive and brittle than PET and would not be suitable for producing plastic bottles like PET is used for. Lastly, compared to PE, PHB has the same tensile strength but lower elongation at break indicating that PHB is less ductile than LDPE and HDPE. While PHB has great potential for biomedical and pharmacological applications, we are focusing on producing PHB use in consumer/food grade packaging and agricultural applications due to our product purity specification.

Table 3.1. Summary of mechanical properties of PHB and petrochemical based polymers (PP, PET, PE) (McAdam et al., 2020).

Mechanical Property	PHB	PP	PET	LDPE	HDPE
Tensile Modulus (GPa)	3−3.5	1.95	9.35	0.26−0.5	0.5−1.1
Tensile Strength (MPa)	20−40	31−45	62	30	30−40
Elongation at break (%)	5−10	50−145	230	200−600	500−700
Degree of Crystallinity (%)	50−60	42.6−58.1	7.97	25−50	60−80
Melting Temperature (°C)	165−175	160−169.1	260	115	135
Glass Transition Temperature (°C)	5−9	-20−-5	67−81	-130−100	-130−100

4. Raw Material: Crude Glycerol

The feedstock to our overall process is crude glycerol, produced as a byproduct from three biodiesel production plants located in Iowa and owned by Renewable Energy Group, Inc. (REG). Crude glycerol quality varies largely across different vendors with a variety of different operational and environmental factors (Sims, 2011). Additionally, due to a lack of disclosed specifications of crude glycerol quality from other vendors, we chose to purchase crude glycerol feedstock from REG exclusively. The commercial crude glycerol sold by REG is within the pH

range of 4-7.5 and is composed as follows: 80 wt% glycerol, 13 wt% moisture, 7 wt% ash, 1 wt% total fatty acid, and 0.3 wt% methanol (MeOH) (*REG Glycerin Fact Sheet*, n.d.).

We chose *Cupriavidus necator* ATCC 17699 as the microbial strain to produce PHB. Tanadchangsaeng & Yu (2012) used this strain to microbially synthesize PHB as it was adapted in a glycerol-rich environment, ensuring effective utilization of glycerol as a carbon source. Under nitrogen limiting conditions, *C. necator* produces large amounts of PHB which can then be separated from the cells and purified downstream.

Along with the crude glycerol, we will feed the system ammonium hydroxide (NH_4OH), sulfuric acid (H_2SO_4), and potassium hydroxide (KOH) as nitrogen sources and pH regulators. We are assuming that the trace amounts of fatty acid and ash in the crude glycerol will supply the microbes all of the micronutrients they need to grow. Lastly, filtered air will be fed into the system as the oxygen source for this aerobic fermentation.

5. PHB Production Plant: Scope and Scale

Our plant will have a PHB production capacity of 7.32 kilotons per annum (ktpa). We chose this scale because we plan to partner with a large biodiesel company to buy all of 29.9 ktpa of their waste glycerol from their biorefineries in Iowa. The Renewable Energy Group is a subsidiary of Chevron that produces biofuels (*Learn About Renewable Energy Group*, n.d.). They have three biodiesel facilities in Iowa located within 150 miles of each other (see Table 5.1 for a breakdown by location) and our PHB production plant will be located equidistant from these three facilities (see Figure 5.1). Sourcing feedstock from one company will ensure a more uniform feedstock as crude glycerol is known to be quite variable (Sims, 2011). The current global PHB production capacity is estimated to be less than 30 ktpa so our plant would represent

around 25% of total production (Posada et al., 2011). Our target market would be plastic extruding companies in the midwest.

Table 5.1. Feedstock Sources for PHB Plant in Iowa *("US Biodiesel Plants," 2022)*

Biodiesel Plant	**Location in Iowa**	**Biodiesel Annual Capacity (ktpa)**	**Glycerol Annual Capacity (ktpa)**
REG Ralston LLC	Ralston	99.55	9.95
REG Newton LLC	Newton	99.55	9.95
REG Mason City LLC	Mason City	99.55	9.95
		Total Supply	29.9

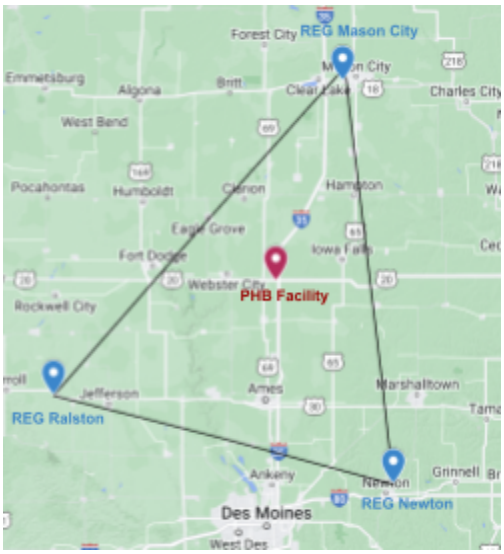

Figure 5.1. Feedstock Sources and PHB Facility Location

6. Upstream Process

6.1. Upstream Process Overview and Theory

Tag	Equipment
CM-101	Air Compressor
S-101	Air Sterilizer
R-101	Seed Fermenter
R-102	Product Fermenter

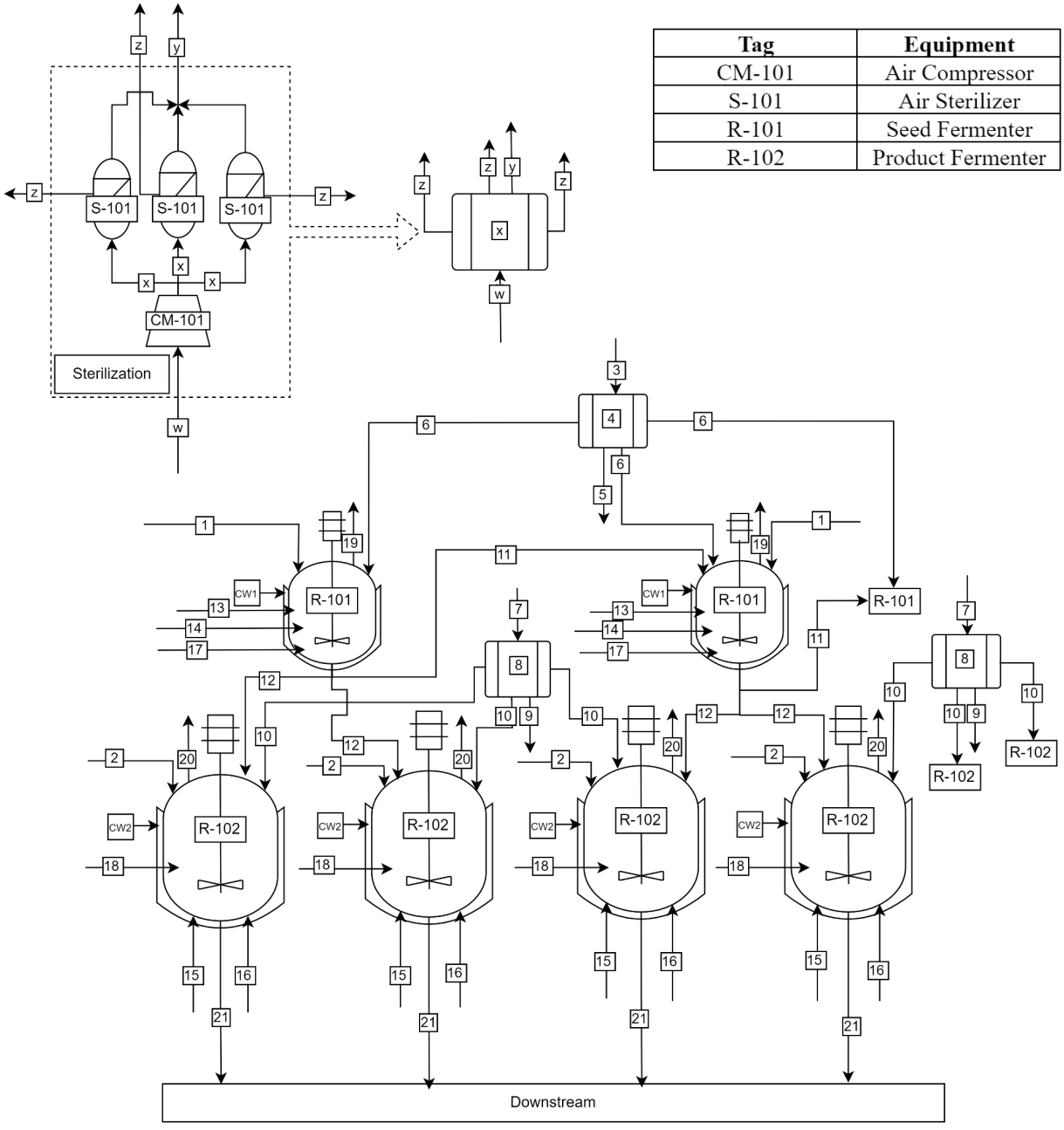

Figure 6.1.1 Upstream Process Flow Diagram (see Appendix I for stream names)

The process flow diagram in Figure 6.1.1 illustrates a subsection of the total upstream process. The quantities in the stream table in Appendix I represent flows per fermentation since the upstream process is fed-batch. Duplicate stream numbers represent identical quantities. In the sterilization block, sufficient air for three fermenters (R-101 or R-102) is compressed in CM-101 and passed through three parallel air filters (S-101) before being fed into the fermenters. For the sake of space and clarity, the sterilization block consisting of the compressor and three air filters is represented by a simplified symbol where the streams denoted by w, x, y, and z correspond to the air, compressed air, vented air, and filtered air streams respectively in each of the sterilization blocks. In the main diagram, these letters are replaced with the respective stream numbers. While three are shown in Figure 6.1.1, there are 11 total sterilization blocks. Two seed fermenters (R-101) are included here to show that each seed fermenter (R-101) feeds two product fermenters (R-102) and one seed fermenter (R-101), which is why four product fermenters (R-102) are also included here. In the full process, there are three groups of three seed fermenters (R-101) and four groups of six product fermenters (R-102) which operate on a schedule detailed in Section 6.2 to meet the plant's target for PHB production.

The goal of the upstream process is to grow *C. necator* in optimal conditions to produce maximum concentrations of PHB that will be isolated later in the downstream process. The fermentation substrate is crude glycerol (80 wt%), a byproduct of biodiesel production. It contains other impurities such as moisture (13 wt%), methanol (0.1%), ash (7 wt%), and total fatty acid (1 wt%), which we determined are a) beneficial for fermentation, b) present in trace amounts, or c) neither beneficial nor detrimental to the process but would be uneconomical to remove them prior to glycerol utilization. Additionally, since the crude glycerol feedstock is

sourced from a biodiesel production process, we determined that our media is free of contamination from other bacteria.

Based on our crude glycerol supply and the *C. necator* productivity, we can produce PHB at a rate of 7.3 ktpa. From the material balances, we determined the upstream raw materials reached a total mass of 332 ktpa, with process water accounting for 209 ktpa of the total. We designed our bioreactors to accommodate for the high influx of raw materials required to produce the target PHB amount while considering the mass transfer limitations of an aerobic fermentation. According to industry standards, the larger end of aerobic fermenter volumes reach 100 m^3 (Meyer & Minas, 2017). With this in mind, we designed a 100 m^3 bioreactor to our target k_La, as described in Section 6.3. Choosing a large bioreactor is necessary to minimize capital costs; instead of purchasing an excessive amount of small-volume fermenters, we are purchasing a moderate amount of large-volume fermenters. Ultimately, the limiting factors for the bioreactor size are the process water volume and PHB production goal. Given the growth kinetics of *C. necator* supported from literature, handling a substantial water supply is necessary to reach our PHB capacity (Cavalheiro et al., 2009).

To ensure that the water supplied for the fermentation process is sterile, we are employing a direct sterilization method, by feeding in water into the sterile fermenter and directly injecting steam. Initially, we considered using an external thermal sterilizer and heat exchanger to cool the water before entering the fermenter; however, we decided a direct sterilization method would be more cost effective as the sterilization and cooling step takes place in a single unit. Additionally, the air supplied to the fermenter will be compressed and fed to a microfiltration unit (S-101) as a sterilization step.

First, *C. necator* will be grown in a seed train (R-101) to provide high cell density inoculum to the large fed batch bioreactors (R-102). Then, this inoculate will be transferred to large fed-batch reactors (R-102) where *C. necator* will be further grown to accumulate PHB. Over the growth phase, *C. necator* grows in the glycerol media and PHB slowly accumulates within the cells' cytoplasm with the supply of nitrogen in the form of ammonium hydroxide. Around two-thirds of the way through the fermentation process, the nitrogen source to the reactor is replaced with potassium hydroxide (KOH), which initiates "nitrogen stress response" and causes the microbes to store mass amounts of substrate (Koch et al., 2019). Then, the microbes produce mass amounts of PHB in the nitrogen depletion phase.

For each fermentation cycle, the cell growth phase occurs for 26 hours, during which nitrogen is supplied, and the PHB accumulation stage occurs for 7.5 hours, during which the nitrogen source is removed and replaced with a KOH solution. At the end of the cell growth phase, the biomass concentration is at 48 g/L, while the PHB concentration is at 4.3 g/L. When this PHB accumulation phase starts, it takes 5 hours for the nitrogen to fully be depleted, but PHB is still accumulating within the cells during this time. At the end of the 7.5 h period, the PHB or product concentration increases to 26 g/L, while the biomass concentration drops to 44 g/L.

Each bioreactor is designed as a fed batch such that the stock solution, along with the acid (H_2SO_4) and ammonium hydroxide (NH_4OH) or potassium hydroxide (KOH) solutions, are fed continuously into the reactor, but not removed until the end of the fermentation period. The volume inside the reactor increases with time as more material is fed in at a constant flow rate, with the initial volume at 74 m^3 and the final volume at 100 m^3 (Figure 6.1.3). In terms of the transient behavior, the fermentation is assumed to follow quasi-steady state behavior, where the

dilution rate (D) is equivalent to the specific growth rate of the cells (μ). The assumption is called 'quasi-steady state' because the cell, substrate, and product concentration is assumed to be steady, but the total volume of the reactor is transient with respect to time (Shuler & Kargi, 2002). The quasi-steady state assumption yields the following differential equations (Equations 6.1.1-5):

$$\frac{dX^t}{dt} = (\mu - \frac{F}{V})X^t \quad 6.1.1$$

$$\frac{dV}{dt} = F \quad 6.1.2$$

$$\frac{dS^t}{dt} = -\frac{1}{Y_{XS}}\mu X^t + S_0 F \quad 6.1.3$$

$$\frac{dP^t}{dt} = \frac{1}{Y_{XP}}\mu X^t \quad 6.1.4$$

$$\mu = \frac{F}{V} \quad 6.1.5$$

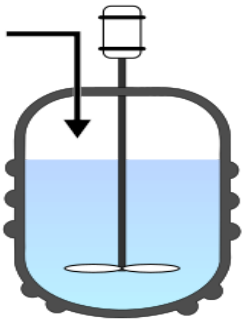

Figure 6.1.2. Fed Batch Fermentation Process

Fermentation behavior can be theoretically modeled by these governing equations, however, empirical data using the same assumptions exists, so that was adapted to model bioreactor design and outline a batch operation schedule. The kinetic data used in this design project is from Cavalheiro et al.'s (2009) study named *Poly(3-hydroxybutyrate) production by Cupriavidus necator using waste glycerol*. In Figure 6.1.2, the total mass of cells and PHB is

plotted vs the time of one fermentation cycle. It is assumed that from quasi-steady state, the concentration of cells and product is constant with respect to time so the total mass is proportional to the change in volume of the fermenter.

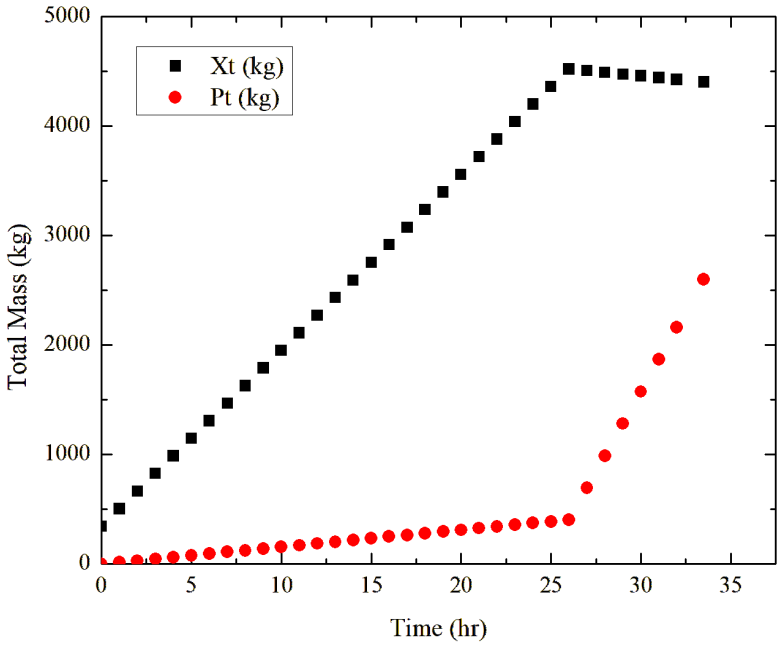

Figure 6.1.3. Total Mass of Cells (Xt) and PHB (Pt) Throughout Fermentation

The kinetic parameters used to model each bioreactor are summarized in Table 6.1.1. Oxygen supply in the reactor is described by specific oxygen uptake rate (q) and the volumetric oxygen mass transfer coefficient (k_La). The specific oxygen uptake rate is the amount of oxygen that is consumed per time per cell mass. It is generally proportional to the cell growth rate and can be obtained by measuring the inlet and outlet gas rate. The volumetric oxygen mass transfer coefficient describes the capacity of oxygen supply and transfer in the fermenter, which depends on parameters such as agitation speed, aeration rate, geometric characteristics of the fermenter, and viscosity of the media (Shuler & Kargi, 2002).

Table 6.1.1. Bioreactor Design Requirements (Cavalheiro et al., 2009)

Parameter	Value
Specific Uptake Rate of O_2 (gO_2 / gX h)	0.005
Min Amount of O_2 Required (mg/L)	$6.6*10^{-3}$
Oxygen Solubility in System (mg/L)	6.6
Biomass Yield, X (g/L)	48.3
Volumetric Transfer Coefficient, k_La (h^{-1})	40.6
Maximum Specific Growth Rate, μ_{max} (h^{-1})	0.15

6.2. Batch Schedule

Using the 30 kilotons per annum (ktpa) crude glycerol supply from neighboring biodiesel plants, our plant will produce over 8 ktpa of PHB. At the time of this capstone, there is limited data available on the microbial kinetics of supplying *C. necator* with crude glycerol to produce PHB; however, one study comparing the use of pure glycerol versus crude glycerol in fed-batch fermentations provides enough empirical data to design an industrial scale fermentation (Cavalheiro et al., 2009). Notably, crude glycerol as a substrate does not have a cell or product yield as favorable as pure glycerol or glucose, so the plant fermentations have to be more dilute than if a better carbon source was used (Cavalheiro et al., 2009; Tanadchangsaeng & Yu, 2012). Given these constraints, the plant requires 24 product fermenters (R-102) with a 100 m^3 working volume to produce 2600 kg PHB per fermentation. Accounting for equipment cleaning and sterilizing, water and inoculate addition, media sterilization, and product broth draining, an entire fermentation cycle is 64 hours.

The first 8 hours of the cycle are dedicated to cleaning in place (CIP) and sterilization in place (SIP), as well as adding the 58 m^3 starting water volume. CIP and SIP are automated processes which streamline equipment cleaning and sterilizing between fermentations because

the fermenter does not have to be taken apart (Marks, 2003). At the scale of this project, the CIP and SIP systems have to be commissioned during plant development and optimized to our unique process (McNulty, 2016). A conservative estimate for the length of our CIP and SIP cycles is 2 hours each, so the rest of the time block is dedicated to adding water to the fermenters. The second 8-hour block is for sterilizing the water using direct steam injection. About 8,700 kg of steam is injected over 1-2 hours to raise the water temperature to 120°C and the media is held at that temperature for 1 hour. During direct steam injection, the total water volume in the fermenter is brought to 67 m^3. Finally, the temperature is decreased over 2 hours to 34°C using the cooling water jacket surrounding the fermenter. The next 2.5 hours are used to load 7.8 m^3 of inoculate from the seed train, and the final half hour is actually the start of the active fed-batch fermentation.

The active fed-batch fermentation takes place over four 8-hour blocks, with an extra half hour in the sterilization block and an extra hour in the unloading block to reach a full 33.5-hour fermentation. During this time, a constant feed of crude glycerol, water, ammonia solution, and aqueous acid enter the fermenter, with the acid used only to maintain pH at 6.8. After 26 hours, the ammonia solution is stopped to initiate nitrogen limitation and replaced with a sodium hydroxide solution to maintain pH. The fermentation ends at 33.5 hours, when the PHB concentration plateaus around 26 g/L (Cavalheiro et al., 2009). The last two 8-hour blocks of the cycle are dedicated to removing the broth from each fermenter to produce a continuous 40,000 L/h downstream flow.

The fermentation cycles are laid out in an 8-day schedule for four groups of six product fermenters (R-102), as shown in Table 6.2.1. The schedule is repeated 44 times per year and results in 96% plant uptime.

Table 6.2.1. Fermentation Batch Schedule

Day	Time	R-101 Group 1	R-101 Group 2	R-101 Group 3		R-102 Group 1	R-102 Group 2	R-102 Group 3	R-102 Group 4
1	0:00	A	A	C		C	A	A	U
1	8:00	U	A	S		S	A	A	U
1	16:00	C	A	A		A	A	U	C
2	0:00	S	U	A		A	A	U	S
2	8:00	A	C	A		A	U	C	A
2	16:00	A	S	U		A	U	S	A
3	0:00	A	A	C		U	C	A	A
3	8:00	U	A	S		U	S	A	A
3	16:00	C	A	A		C	A	A	U
4	0:00	S	U	A		S	A	A	U
4	8:00	A	C	A		A	A	U	C
4	16:00	A	S	U		A	A	U	S
5	0:00	A	A	C		A	U	C	A
5	8:00	U	A	S		A	U	S	A
5	16:00	C	A	A		U	C	A	A
6	0:00	S	U	A		U	S	A	A
6	8:00	A	C	A		C	A	A	U
6	16:00	A	S	U		S	A	A	U
7	0:00	A	A	C		A	A	U	C
7	8:00	U	A	S		A	A	U	S
7	16:00	C	A	A		A	U	C	A
8	0:00	S	U	A		A	U	S	A
8	8:00	A	C	A		U	C	A	A
8	16:00	A	S	U		U	S	A	A

C	Automated cleaning/sterilizing and water addition
S	Water sterilization and inoculate addition
A	Active fed-batch fermentation
U	Remove PHB accumulated broth

The seed fermenters (R-101) follow a similar schedule as the product fermenters (R-102) and require the same cleaning and sterilization procedures. The deviations from the product fermenter (R-102) schedule are the fermentation length and the unloading time. The fermentation only requires 26 hours to reach a maximum cell density of 48 g_{DW}/L because the intention is for the broth to be a high cell density inoculate. The extra two hours that do not fit within the three dedicated 8 hour blocks are covered by the sterilization and unloading block, as these do not require as much time for a smaller volume fermenter. The unloading time only requires an 8-hour block because the seed fermenters (R-101) will be drained in parallel to inoculate the product fermenters (R-102) and the next seed fermenter (R-101) group. With these changes, the plant needs nine seed fermenters (R-101) with a 16 m^3 working volume, divided into three groups (Table 6.2.1).

6.3. Bioreactor Design

When designing the fermentation process, we considered using two bioreactors per fed batch fermentation, with one dedicated to the growth phase and the other dedicated to the accumulation phase. Essentially, the cells would be grown in one fermenter with nitrogen and pumped to the next fermenter to accumulate PHB in the absence of nitrogen. We determined that spending time pumping the bioreactor contents from one vessel to the next is not needed and trace amounts of cells or PHB could be lost in the transport process. Beyond that, we also consulted industry fermentation processes, which effectively function with using one bioreactor per fermentation. In this design, nitrogen would be adequately supplied for cell growth and removed and replaced by another basic solution to initiate the accumulation phase. Originally, we intended to use 12 200,000L fermenters to grow our cells. Consulting with Professor Prpich, we believed it to be physically feasible to use such large fermenters. However, after considering

the economics of purchasing double the amount of smaller bioreactors, we found it more economically feasible to purchase 24 100,000 L bioreactors. This number and size of fermenters is necessary to reach the target PHB production. The bioreactor design was centered around supplying enough oxygen to the cells to maximize cell growth (Table 6.1.1). Using lab scale data, we calculated our target k_La to be 40.6 h^{-1} (see Equation 6.3.4), and designed the 100,000 L working volume bioreactor to meet this specification. In industry there are other universal rules used for bioreactor design that are provided below in Table 6.3.1. These equations ensure that the system can meet the oxygenation requirements of the cells while also not overloading the system with issues such as flooding or slugging of the reactor. Flooding occurs when bubbles under the impeller coalesce together because the shear rate of the impeller is too low. Slugging is similar but occurs when the tip speed of the impeller is too high and causes air pockets to form (Shuler & Kargi, 2002).

Table 6.3.1 Bioreactor Design Rules (Shuler & Kargi, 2002)

Variable	**Equation**	**Specification to meet**
Superficial velocity (v_s)	$v_s = \frac{Q_g}{\pi D_t^2/4}$	v_s < 125 m/h to prevent slugging
Volumetric Aeration Rate (Q_g)	$Q_g \leq 0.6\,(\frac{D_i^5 N^2}{D_t^{1.5}})$	Prevents gas flooding
Number of Impellers (n_i)	$\frac{H_l - D_i}{D_i} \geq n_i \geq \frac{H_l - 2D_i}{D_i}$	
Tip Speed	Tip speed = $\pi N D_i$	Tip speed > 2.5 m/s for good gas dispersion
Ratio of Power Input of Gassed System to Tank Volume	$\frac{P_g}{V}$	$\frac{P_g}{V} < 15,000\ \frac{W}{m^3}$

To design the bioreactor to meet the kLa requirements of the system and the industry standard practices, the following design process was taken. First, an initial estimation of appropriate volumetric aeration rates and impeller speed was made from the working volume of the bioreactor. Q_g values usually fall within 0.3-1 vessel volumes per minute (vvm) and for bioreactors larger than 10,000 L, N is usually between 25-200 rpm. Next, the geometry of the tank was determined. A non-standard geometry was assumed where the liquid height of the tank was three times that of the diameter. This geometry is common with large bioreactors to limit tip speed (Meyer & Minas, n.d.). The diameter of the impeller was sized to be half of the tank diameter. These initial values were used to calculate the Reynold's number of the fluid in the tank (see Equation 6.3.1).

$$Reynold's\ Number\ (Re) = \frac{\rho D_i^2 N}{\mu} \quad 6.3.1$$

The calculated Reynold's Number was then used to calculate the power number (N_P) of the system. N_P was calculated with the following correlation, assuming that the bioreactor would be using a flat six-blade turbine (rushton turbine) with four baffles (see Figure 6.3.1).

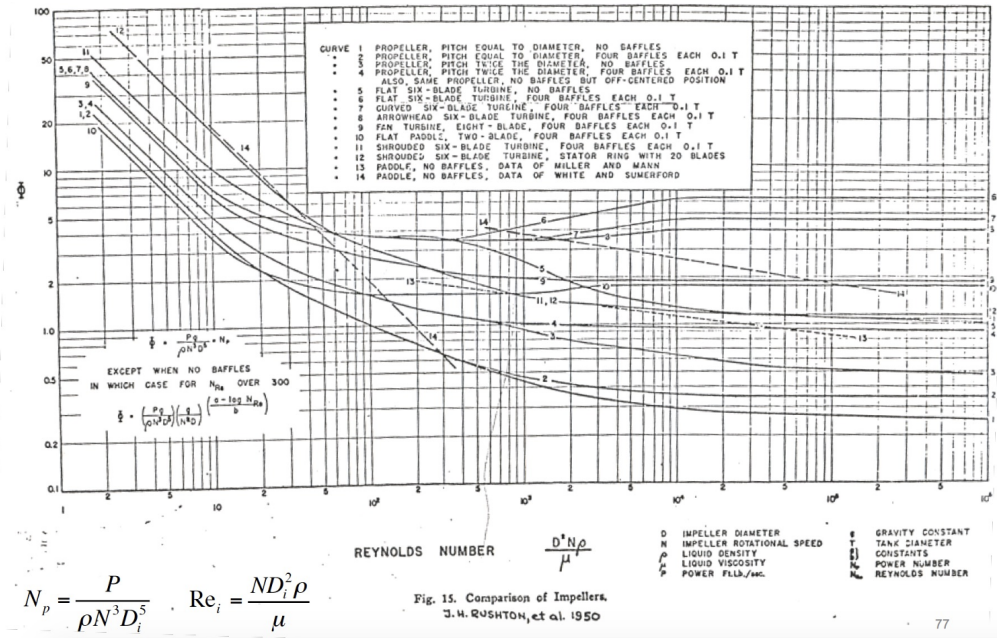

Figure 6.3.1. Power Number (Np) Correlation (Rushton et al., 1950)

Using N_P, the ungassed power requirement (P) of the reactor was calculated using Equation 6.3.2. P represents the power required to spin the agitator in an non-aerated bioreactor.

$$P = N_p \rho N^3 D_i^5 \, [W] \quad 6.3.2$$

Next to calculate the gassed power requirement of the system (P_g), the aeration number was calculated using Equation 6.3.3.

$$N_a = \frac{Q_g}{ND_i^3} \quad 6.3.3$$

Then the gassed power to ungassed power ratio was found using the correlation below assuming the rushton turbine correlated with line A (see Figure 6.3.2)

$$N_a = \frac{Q_g}{ND_i^3}$$

A: Flat-blade turbine (n_p=8)
B: Vaned disk (n_p=8)
C: Vaned disk (n_p=6)
D: Vaned disk (n_p=16)
E: Vaned disk (n_p=4)
F: Paddle
D_t/D_1=3
W_b/D_t=0.1
D_t/H_1=3

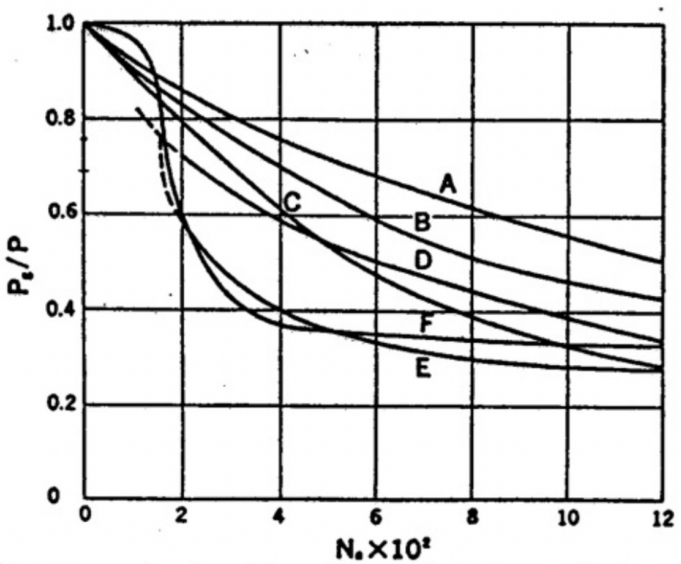

Power requirements for agitation in a gassed system. The ordinate and abscissa are the degree of power decrease, P_g/P, and the aeration number, N_a. Parameters are the types of impellers, whose representative geometrical ratios in agitated vessels are also shown in the figure.[38]

Figure 6.3.2. Gassed to Ungassed Power Correlation (Rushton et al., 1950)

Lastly, the k_La of the bioreactor was calculated using Equation 6.3.4 which is an empirically derived formula.

$$k_L a = \frac{0.0333}{D_t^4}\left(\frac{P_g}{V}\right)^{0.541} Q_g^{0.541/\sqrt{D_t}} \quad 6.3.4$$

This process was iterated changing Qg and N until the calculated k_La was within 10% of the target k_La.

A summary of the bioreactor design specifications is shown below in Table 6.3.2

Table 6.3.2. Product Bioreactor Schematics and Operating Conditions

Parameter	Value
Temperature (°C)	34
Reactor Volume (L)	175,000
Liquid Volume (L)	100,000
Tank Area (m^2)	9.5
Tank Height (m)	19
Tank Diameter (m)	3.5
Impeller Diameter (m)	1.75
Impeller Spacing (m)	2
Impeller Type	Rushton Baffled Impellers
Number of Impellers	4
k_La (h^{-1})	42
RPM	80
Air Supply (vvm)	0.5
Reynold's number	Turbulent Range
Pg/V (W/m^3)	11,000

6.4. Seed Train Design

In the upstream process, a culture of *C. necator* is first grown within a seed train. The purpose of a seed train is to provide a high density inoculum volume to large scale bioreactors. For the seed train, we considered using wave bioreactors, which operate by rocking the system at a constant speed or angle to allow for oxygen transfer and cell growth. After researching further, we found that the largest volume capacity of wave bioreactors available was 1000 L, which would require that we purchase numerous units. Furthermore, wave bioreactors do not allow for adequate oxygen transfer when compared to stirred tank bioreactors due to their scale. Based on

these considerations, stirred tank bioreactors were employed in the seed train. In the seed train, there will be three groups of three fermenters. In reference to capacity, each fermenter in the seed train is designed to have a working volume of 16,000 L. Based on the growth kinetics of *C. necator*, the initial mass of cells needed for each product fermenter (R-102) was found to be ~344 kg. Using this, the inoculum volume needed for each product fermenter (R-102) was calculated to be ~7100 L. Each seed fermenter (R-101) produces enough cells to inoculate two product fermenters (R-102) and one seed fermenter (R-101). The solids produced in each seed fermenter (R-101) are mainly biomass, as nitrogen is readily available throughout fermentation. Based on the growth kinetics of *C.necator*, the initial mass of cells needed for each seed fermenter (R-101) is ~77.3 kg. The final mass of cells is 773 kg for the 16,000 L seed train fermenters (R-101).

In reference to material balance calculations for the seed train, ~30 ktpa of crude glycerol is fed to the overall fermentation process, with a portion going to the seed train to cultivate cell culture, and returning back to the product fermentation. The product fermenter (R-102) is designed to have 100,000 L working volume, while the seed fermenter (R-101) has a 16,000 L working volume. This ratio of seed (R-101) to product fermenter (R-102) volume (0.16) was used to determine stream flow rates (Appendix I).

The operating design and schematics for the seed fermenter (R-101) used the same theoretical background as the design of the product fermenter (R-102). Because the working volume is smaller, the power requirement decreases in magnitude. However, the design requirement that remains the same across both bioreactors is the k_La. The operating temperature and pH also remains the same. As a note, the impellers in both fermenters will be vertically spaced. A summary of the design and operation conditions are provided in Table 6.4.1.

Table 6.4.1 Seed Train Bioreactor Operating Design and Schematics

Parameter	Value
Temperature (°C)	34
Reactor Volume (L)	30,000
Liquid Volume (L)	16,000
Tank Area (m^2)	5.9
Tank Height (m)	5.2
Tank Diameter (m)	2.7
Impeller Diameter (m)	0.91
Impeller Spacing (m)	1.5
Impeller Type	Rushton Baffled Impellers
Number of Impellers	2
k_La (h^{-1})	42
RPM	105
Air Supply (vvm)	0.5
Reynold's number	Turbulent Range
Pg/V (W/m^3)	2,200

6.5. Fermentation Air Sterilization

The air fed to the upstream process will be sterilized before being used in the seed train and bioreactor. Air at ambient conditions will first be fed at a rate of 1700 kg/hr to a compressor and reach a temperature of 178.5℃ and pressure of approximately 308,000 Pa. From ASPEN simulations, we determined that the volumetric flow rate of compressed air fed to the filter is approximately 720,000 L/hr. This compressed air flow will split into 3 streams and feed 180,000 L/hr to each filter. Each fermenter will have its own filter, resulting in a total of 33 filters. The polytetrafluoroethylene (PTFE) filters we will purchase from Global Filter have a rating of 0.2

μm (see Table 6.5.1). Bacteria size is generally within the range of 0.2 to 60 microns (Osmonics Inc, 1996). We assumed the filter to have a rejection rate of 1%, so that 561 kg/hr is fed to both the seed train and bioreactors, meeting the oxygen requirements discussed in the previous sections regarding bioreactor design. The 1% amount of fed air that is not filtered will be vented to the atmosphere. The compressors and air filters for both the seed and product fermenters have identical design because the hourly flow rate of air into all of the fermenters is the same, although the per fermentation quantities are different (see Appendix I).

To determine the pressure drop of the filter, we referred to the flow rate, in standard cubic feet per minute (SCFM) and pressure drop (psi) data given by Global Filter (Global Filter, n.d.). Thus, the actual flow rate of 180,000 L/hr, or 141 actual cubic feet per minute (ACFM) under the conditions leaving the compressor, was used to calculate the flow rate under standard conditions using Equation 6.5.1. Relative humidity, Φ, was assumed to be 0. Pressure terms were in units of psia and temperature terms were in Rankine.

$$ACFM = SCFM * \frac{P_{standard}}{P_{actual} - P_{saturation} * \phi} * \frac{T_{actual}}{T_{standard}} \quad 7.5.1$$

We determined that an actual feed flow rate of 141 ft^3/min is approximately 277 ft^3/min under standard, ambient conditions. Using the data given by Global Filter, at pressure condition 30 psig, a feed flow rate of 277 standard cubic feet per minute (SCFM) results in a pressure drop of approximately 3 psi, or about 20,700 Pa across the filter column (Global Filter, n.d.). It should be noted that the filtration data provided was collected from testing with a 10 inch cartridge. After passing through the filter, the air will still be sufficiently pressurized to be fed into either R-101 or R-102.

Table 6.5.1 Global Filter BRPTFE-Series High Purity Bio-Reduction Grade PTFE Filter Cartridge Specifications (Global Filter, n.d.)

Parameter	Value
Rating (μ)	0.2
Membrane Material	Polytetrafluoroethylene (PTFE)
Length (cm)	102
Outside Diameter (cm)	7
Feed Flow Rate (L/hr)	180,000
Pressure Drop (Pa)	20,700
Change Out ΔP (Pa)	241,000
Maximum Differential Pressure (Pa)	345,000

6.6. Bioreactor Cooling

During aerobic metabolism, the energy stored in the glycerol that is not converted to biological energy by *C. necator* is released as heat. This can raise the temperature in the bioreactor above the design temperature of 34°C, so each bioreactor must be equipped with a cooling mechanism. We primarily considered two types of vessel heat transfer surfaces: an external jacket and vertical baffle coils. Vertical baffle coils increase the heat transfer surface area relative to a simple external jacket. However, as they would also make the cleaning process much more intensive, we proceeded with the external cooling jacket.

The metabolic heat evolved per gram of cell mass, $1/Y_H$ (kJ/g cells), can be determined from the heat of combustion of the substrate, ΔH_s (kJ/g substrate), the heat of combustion of the cells, ΔH_c (kJ/g cells), and the substrate yield coefficient, $Y_{X/S}$ (g cell/g substrate) in Equation 6.6.1. The heat of combustion of glycerol is 17.98 kJ/g glycerol (Cressman et al., 2010). Due to a lack of data on the empirical formula of *C. necator*, we assumed ΔH_C to be 22.5 kJ/g cell, the

average of the range of typical values for the heat of combustion of cells from Schuler and Kargi (2002). $Y_{X/S}$ is 0.45 g cell/g glycerol. The metabolic heat along with the liquid volume in the bioreactor, V_L, the net specific growth rate, μ_{net}, and the cell concentration, X, were used in Equation 6.6.2 to determine the total rate of heat evolution, Q_{GR} during a fermentation, which is ultimately used to calculate the cooling water requirement.

$$\frac{1}{Y_H} = \frac{\Delta H_s - Y_{X/S}\Delta H_c}{Y_{X/S}} \qquad 6.6.1$$

$$Q_{GR} = V_L \mu_{net} X \frac{1}{Y_H} \qquad 6.6.2$$

Note that Q_{GR} is the total rate, meaning that it is calculated using peak values from the end of the growth phase. That is, the maximum heat transfer rate in each bioreactor is around 11.8 million kJ/hr, or 35 kJ/m^3 on a per volume basis. In our fed-batch system, V_L is taken to be a function of time such that Q_{GR} can also be considered as a function of time. We used the maximum Q_{GR} to design the cooling water jacket. The cooling jacket was assumed to be similar in configuration to a single-pass double pipe heat exchanger, with the exceptions that the cooling water is the only moving fluid and the fluid temperature inside the bioreactor should be constant. To mitigate any temperature increase due to Q_{GR}, we determined the required inlet water temperature, $T_{C,in}$, and flow rate, m_C, such that both Equations 6.6.3 and 6.6.4 were satisfied.

$$Q_t = m_C C_{p,C}(T_{C,out} - T_{C,in}) \qquad 6.6.3$$

$$Q_t = U_o A_o \Delta T_{lm} \qquad 6.6.4$$

$C_{p,C}$ is the heat capacity of the cooling water and $T_{C,out}$ is the exiting cooling water temperature. A_o is the inner contact area inside the fermenter and ΔT_{lm} is the logarithmic mean

temperature difference. We assumed that the conductive heat transfer in the bioreactor wall and the convective heat transfer from the cooling water to the wall are negligible compared to the convective heat transfer within the bioreactor. Therefore, the overall heat transfer coefficient, U_o, is governed by the heat transfer coefficient of the inner fluid, h_i, as seen in Equation 6.6.5. The Nusselt number correlation for heat transfer between a fluid and a jacketed wall (Equation 6.6.6) was used to calculate h_i, in which we assumed the ratio of the bulk and surface densities μ/μ_s to be equal to unity and *a* and *b* are constants for a disc or flat-blade turbine obtained from Table 18-1 in *Perry's Chemical Engineers' Handbook*, 9th edition (Green, 2018). The Reynolds (Re) number and Prandtl (Pr) are given by Equations 6.6.7 and 6.6.8.

$$U_o = \frac{r_i h_i}{r_o} \qquad 6.6.5$$

$$Nu = \frac{h_i D_T}{k} = aRe^b Pr^{1/3} \left(\frac{\mu}{\mu_s}\right)^{m'} \qquad 6.6.6$$

$$Re = \frac{N D_i^2}{\nu} \qquad 6.6.7$$

$$Pr = \frac{\nu}{\alpha} = \frac{\mu C_p}{k} \qquad 6.6.8$$

Calculation of the inner heat transfer coefficient requires the thermal conductivity, *k*, of the cell slurry within the bioreactor. To estimate this value, we found the thermal conductivity of a sugar solution with a similar viscosity to that of our cell slurry. The viscosity of our cell slurry was approximated as that of *E. coli* cell broth, which is around 20 cP (Carta, 2021). In order for the heat transfer rate Q_t in Equations 6.6.3 and 6.6.4 to be equal to Q_{GR}, each bioreactor requires an inlet cooling water temperature of 15°C. The required cooling water flow rate increases from around 24 m^3/hr up to a maximum of 318 m^3/hr as the microbes grow throughout the fermentation. As the seed train is essentially a scaled down version of the product bioreactors,

they also require cooling jackets. We calculated the cooling requirement for the smaller bioreactors by accounting for their different geometry in the heat transfer area and working volume.

7. Downstream Process

7.1. Downstream Process Overview

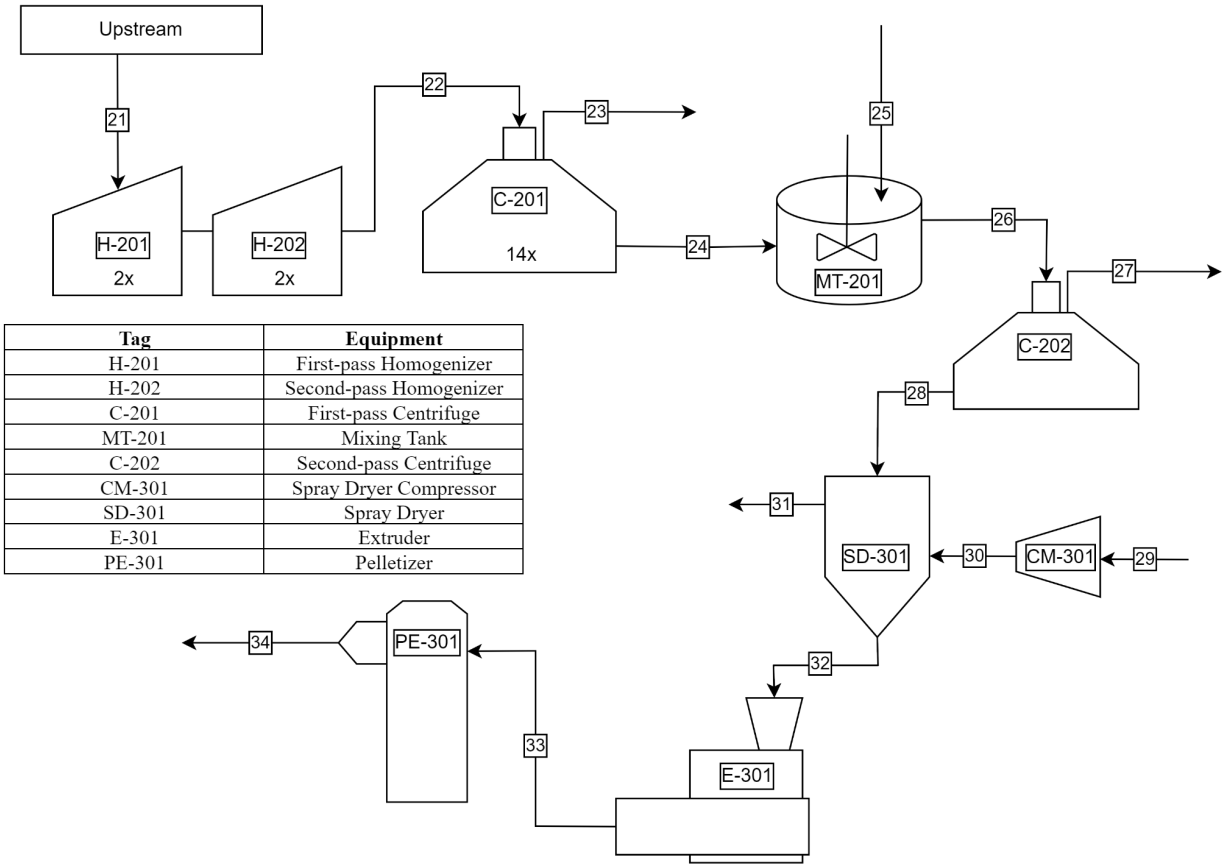

Tag	Equipment
H-201	First-pass Homogenizer
H-202	Second-pass Homogenizer
C-201	First-pass Centrifuge
MT-201	Mixing Tank
C-202	Second-pass Centrifuge
CM-301	Spray Dryer Compressor
SD-301	Spray Dryer
E-301	Extruder
PE-301	Pelletizer

Figure 7.1.1 Downstream Process Flow Diagram (see Appendix II for stream names)

The goal of the downstream process is to separate, purify, and package the PHB to be sold to plastic manufacturers. First the fermenter effluent is sent through two homogenizers to perform cell lysis. Then the disrupted cells are sent through a series of two disc-stack centrifuges for isolation of the PHB product. Between centrifugation steps, there is an intermediate mixing

step for resuspension of the PHB. Then the PHB and water mixture is sent through a spray dryer and the 99.2% pure PHB is then sent through a plastic extrusion process to produce 25 kg bags of 3mm plastic pellets.

7.2. Cell Lysis

The *C. necator* cells must be lysed to release the PHB granules from their cytoplasm. We initially considered solvent extraction using diethyl succinate (DES) which has been found to achieve near 100% PHB purity, though with a relatively low recovery of 90% (Jacquel et al., 2008). DES is also a non-halogenated solvent, making it more environmentally safe and less dangerous for human operators. However, due to the large scale of our operation, extraction with DES would not be economically feasible despite its advantages. To avoid having to purchase large quantities of solvent or detergent, we determined that mechanical lysis is the most applicable method. The two primary mechanical lysis methods are solid shear via a bead mill and liquid shear via high pressure homogenization (HPH). HPH is one of the most widely used cell lysis methods at an industrial scale (Harrison, 1991). We proceeded with HPH over the more lab-scale bead mill.

Homogenization creates a high shear by forcing a large amount of material through a small valve, which lyses the cells. For successful homogenization, there are limits on the viscosity and concentration of the biomass slurry that can be processed (Tamer & Moo-Young, 1998). The biomass concentration of the spent broth from the upstream process has a biomass concentration of 44 g/L, which falls in the allowable range reported by Tamer et al. For this reason, the spent broth can be fed directly into homogenization without an intermediate centrifugation step. According to a study by Ghatnekar et al. (2002), a homogenization pressure of 400 kg cm^{-2}, or 39.2 MPa, with two total passes achieves near complete cell disruption and

release of PHB, allowing for 95% final recovery. Table 7.2.1 summarizes the parameters of the SPX Flow APV Homogenizer Rannie 275Q, which can achieve the required pressure at a high flow rate (SPX FLOW, 2017a).

Table 7.2.1 SPX Flow APV Homogenizer Rannie 275Q Specifications (SPX FLOW, 2017a).

Parameter	Value
Maximum Capacity (L/h)	20,000
Operating Pressure (MPa)	40
Number of Passes	2
Temperature Increase (°C)	8.5
Dimensions (m x m x m)	3.48 x 2.15 x 1.03
Power Requirement (kW)	218

Two homogenizers in parallel are required to process the total flow for 40,000 L/h from upstream. The second pass will occur through a second set of homogenizers. Following homogenization, the higher density of the released PHB relative to the surrounding slurry can be used to isolate it from the slurry.

7.3. Centrifugation

The centrifugation process was split into two parts, with an intermediate mixing step. The first centrifugation step will be performed to remove a majority of the cell debris and water. The intermediate mixing step was included to resuspend the solids prior to the second centrifugation step, which will then remove any residual cell debris from the first centrifugation step. For both centrifugation steps, a 96% efficiency of water and cell debris removal was assumed. (Cambiella et al., 2006).

Initial Centrifugation

For the initial centrifugation step, a centrifuge was designed given the resulting physical properties following homogenization, listed in Table 7.3.1, and the total volume per hour required to be processed. The PHB granules were assumed to be spherical and the fluid density was estimated to be the same as that of water due to the high water content. Cell debris has a density similar to that of water. Vadlja et al. reported the general footprint areas for PHB granules to be in the range of 0.01 to 1.2 μm^2, and from this range we determined the particle radius (Vadlja et al., 2016). The fluid viscosity was approximated to be the same as that of *E. coli* homogenate, which is 0.04 Pa*s (Carta, 2022). The density of PHB granules is 1220 kg/m^3 (*Polyhydroxybutyrate*, n.d.). These physical properties were used to determine the sedimentation velocity, v_g, using Equation 7.3.1.

$$v_g = \frac{4r_p^2(\rho_p - \rho_f)g}{18\eta} \qquad 7.3.1$$

Table 7.3.1 Stream Physical Properties for Initial Centrifugation Design

Physical Property	**Value**
Particle Radius, r_p (m)	$6.18*10^{-7}$
Particle Density, ρ_p (kg/m^3)	1220
Fluid Density, ρ_f (kg/m^3)	1000
Fluid Viscosity, η (Pa*s)	0.04
Sedimentation Velocity, v_g (m/s)	$4.6*10^{-9}$

Disc stack centrifuge parameters were obtained from Table 18-16 in *Perry's Chemical Engineers' Handbook*, 9th edition (Green, 2018). Given the calculated sedimentation velocity and that 40,000 L/h must be processed, the required sigma factor, Σ_T, was calculated using Equation 7.3.2.

$$\Sigma_T = \frac{2\pi(n-1)\omega^2}{3g} cot\ \theta(R_o^3 - R_i^3) \qquad 7.3.2$$

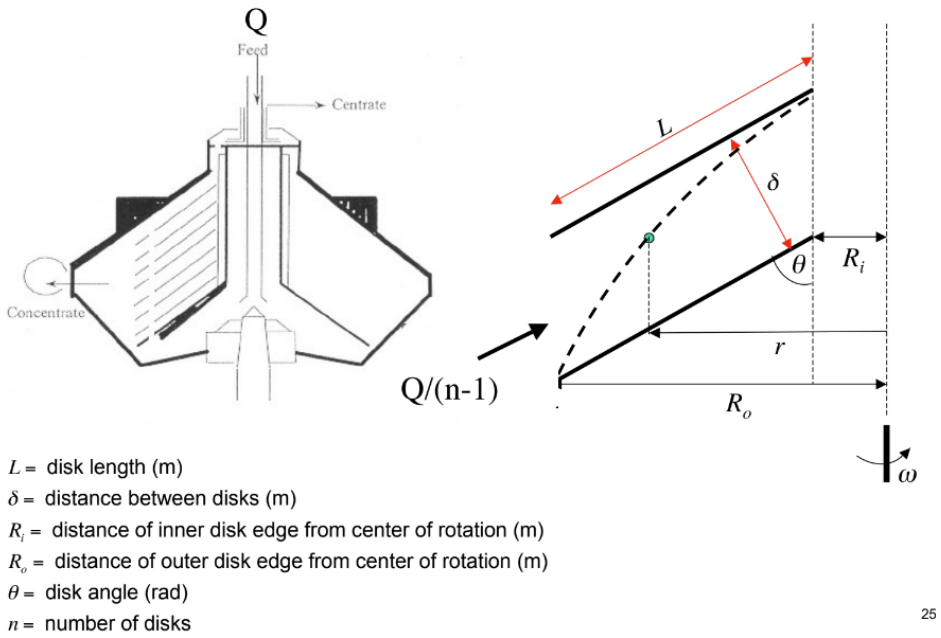

Figure 7.3.1 Disk Stack Centrifuge Diagram (Carta, 2022)

The initial centrifugation step will require 14 disc stack centrifuges with a bowl diameter of 0.61 meters, and other parameters listed in Table 7.3.2 corresponding to the diagram in Figure 7.3.1. They will be continuously operated in parallel to process the total volume per hour of 40,000 L/h.

Table 7.3.2 Initial Centrifuge Design

Parameter	Value
Inner Distance, R_i (m)	0.1
Outer Distance, R_o (m)	0.3
Bowl Diameter, D (m)	0.61
Disc Length, L (m)	0.31
Number of Discs, n	150
Disc Angle, θ (°)	40
Spacing Between Discs, δ (mm)	0.4
Speed (rpm)	4000
Flow Rate, Q (L/h)	2900
Sigma Factor, Σ (m^2)	170000
Maximum Centrifugal Force (g)	5500
Motor Size (kW)	5.9

Following sedimentation, the wet PHB granules with a water content of 60 wt% will be continuously discharged through the nozzles at the periphery of the centrifuge bowl. There will be 24 nozzles due to the large throughput handled by this centrifuge and each nozzle will have a diameter of 3 mm which is sufficiently larger than the PHB granule size.

PHB Solid Resuspension

To resuspend the wet PHB solids discharged from the initial centrifugation step and further dislodge any remaining cell debris, the wet solids will be fed at a rate of 2500 L/h to an intermediate mixing tank with design parameters listed in Table 7.3.3. The tank will also be diluted with water fed in at a flow rate of 7200 L/h, resulting in a total exit flow rate of 9700 L/h and 90 wt% water content.

Table 7.3.3 PHB Solid Resuspension Tank Design

Parameter	Value
Working Volume (L)	6000
Tank Volume (L)	10000
Tank Height (m)	3
Residence Time (min)	37
Mixing Time Factor, nt_T	140
Mixing Time, t_T (s)	84
Tank Diameter, D_t (m)	1.97
Liquid Height (m)	1.97
Mixing Speed (rpm)	100
Impeller Diameter, D_i (m)	0.66
Reynold's Number, Re	$7.2*10^5$
Power number, N_p	0.9
Power, P (W)	510

The mixing tank will operate continuously, so we ensured that the residence time in the tank was longer than the mixing time. Figure 7.3.2 gives the mixing time factor, nt_T, which can be divided by the speed in rotations per second to determine the mixing time required for homogeneity. With a total flow rate into and out of the mixing tank of 9700 L/h and a liquid volume in the tank of 6000 L, the residence time will be 37 minutes. This is much greater than the minimum required mixing time of 84 seconds. We assumed a standard geometry mixing tank with a propeller where the tank diameter, D_t, is three times as large as the impeller diameter, D_a. Additionally, we determined the power required using the same method used for the bioreactor design section.

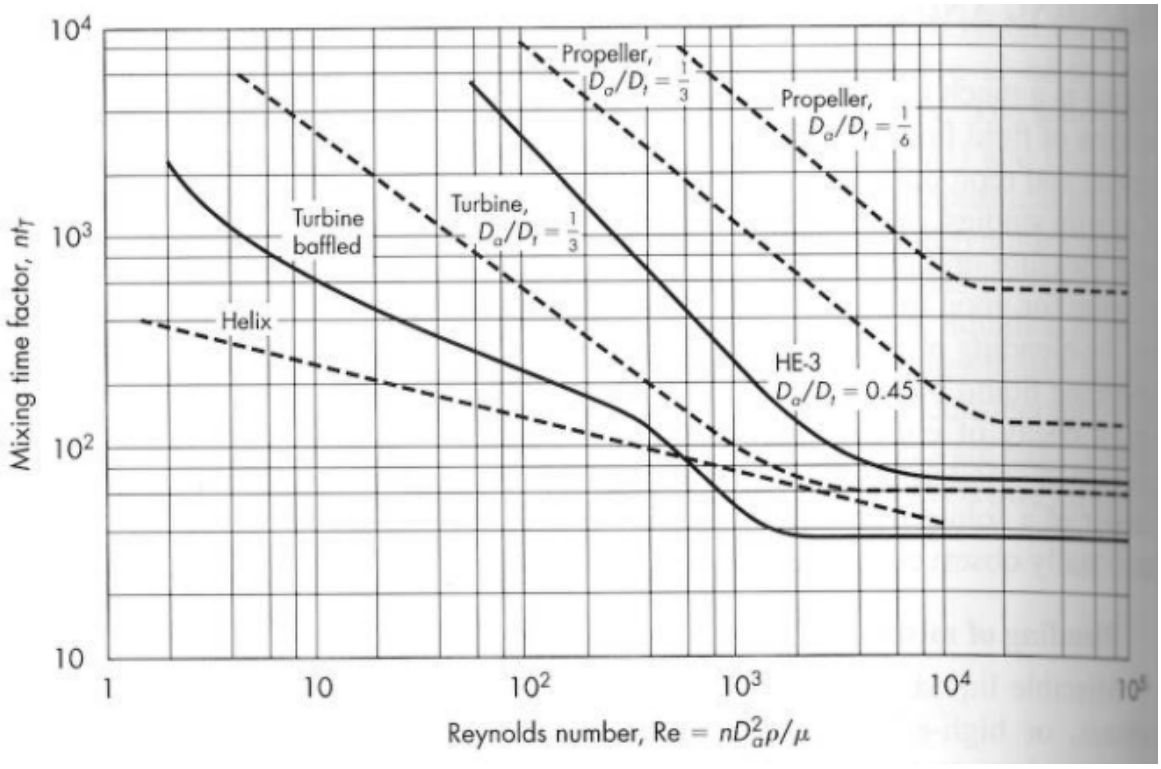

Figure 7.3.2. Mixing Time Factor (nt_T) Correlation (McCabe, 1993)

Final Centrifugation

The contents of the mixing tank are pumped to another smaller centrifuge to once again separate the water. We followed the same procedure for the design of this centrifuge. The key difference in the requirements for this centrifuge is the viscosity, which is much lower now that a majority of the DNA has been removed and the fluid viscosity can be assumed to be that of water (0.001 Pa*s). This lower viscosity resulted in a smaller centrifuge with a higher throughput capacity, allowing the total outlet stream from the mixing tank to be processed by a single centrifuge. The design parameters are listed in Table 7.3.4. The wet solids discharged from this centrifuge have a water content of around 29 wt%.

Table 7.3.4. Second Centrifuge Design

Parameter	Value
Inner Distance, R_i (m)	0.05
Outer Distance, R_o (m)	0.15
Bowl Diameter, D (m)	0.33
Disc Length, L (m)	0.16
Number of Discs, n	150
Disc Angle, θ (°)	40
Spacing Between Discs, δ (mm)	0.4
Sedimentation Velocity, v_g (m/s)	$1.83*10^{-7}$
Speed (rpm)	3500
Flow Rate, Q (L/h)	9700
Sigma Factor, Σ (m^2)	16500
Maximum Centrifugal Force (g)	4300
Motor Size (kW)	4.5

7.4. Spray Drying

Spray drying is used to remove most of the water from the PHB slurry to produce a PHB powder at >99 wt% purity. The spray drying process requires an atomizer to produce fine particles of the solid slurry. The colloidal stream enters the spray dryer along with a flow of hot air. The heat from the air evaporates the moisture from the particles throughout the residence time in the dryer. Dry PHB powder and a moist air stream exit the spray dryer. The dry powder continues to the extruder while the moist air is vented to the atmosphere.

We used Aspen to model the spray drying process. We calculated the heat duty required to evaporate the water from the PHB slurry and used it to determine the required air flow. Before the air enters the spray dryer, it passes through a compressor to reach an absolute pressure of 2.5 atm and temperature of 148℃. The temperature was chosen for two reasons: it is below the

melting point of PHB to ensure the particles remain in solid form, and it is the point at which the tradeoff between heat duty and water removed is optimized (Bushnaq et al., 2022). A compressor is necessary to reduce the volume of air that is sent through the spray dryer which is operating at 1 atm. Sending 7168 kg/hr of 148℃ dry air through the spray dryer results in an exit dry PHB stream of 870 kg/hr at 99.2% purity (see Appendix II and Figure 7.4.1).

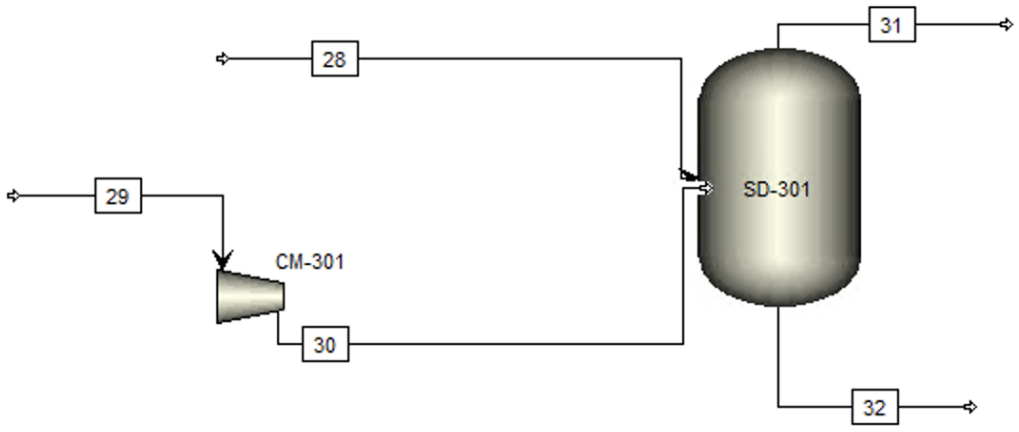

Figure 7.4.1. Spray Dryer Process Flow Diagram

To achieve this separation we need two pieces of equipment: the spray dryer and the atomizer. We chose the SPX Anhydro spray dryer because they produce smaller scale spray dryers for pilot size plants (see Figure 7.4.2). We need a spray dryer with the ability to evaporate approximately 350 kg/hour of water and SPX designs spray dryers ranging from 1-500 kg water/hour. While other specifications of the spray dryer were not available, we chose this manufacturer because of the scalability, easy cleaning design, and process control system of these spray dryers (SPX FLOW, 2017b).

Figure 7.4.2. Pilot Scale SPX Anhydro Spray Dryer

This spray drying chamber will be fitted with a Komline Sanderson Model 860 Rotary Atomizer. We chose this spray dryer because its maximum feed capacity is greater than the expected 5 m^3/h of PHB slurry that will enter the spray dryer. The atomizer will be installed at the top of the drying chamber (*Rotary Atomizer | Komline-Sanderson*, n.d.).

Table 7.4.1. Komline Sanderson Model 860 Rotary Atomizer Specifications

Parameter	**Value**
Maximum PHB Capacity (m^3/h)	6.8
Power Output (kW)	45
Maximum Speed (rpm)	15,000
Atomizer Wheel Diameter (mm)	200
Atomizer Weight (kg)	125

7.5. Extruder

The general purpose of the extruder is to deform a material and shape it with the use of a die (Ek & Ganjyal, 2020). Essentially, the extruder operates at a high temperature such that the material is melted and force is applied to move the material through the die and form the desired shape of the extrudate (Ek & Ganjyal, 2020). There are two types of commonly used extruders,

single and twin screw extruders. Single screw extruders are popular for plastic applications, while twin screw extruders are used in devolatilization or ingredient mixing purposes. The dry PHB powder, exiting the spray dryer, will be fed to the extruder where heat and pressure are applied to transform the powder. For this case, we will mold the powder into 67 homogeneous polymer strands, which will then be cut into pellets using the strand pelletizer. We are purchasing an industrial scale single screw extruder for processing the PHB from Phoenix Equipment Corporation (PEC). The extruder's capacity is 23,500 lb/hr, which is equivalent to ~10,700 kg/hr. Based on the flow for the final processing units (~870 kg/hr), one extruder unit will be purchased to process this PHB flow. The PEC extruder specifications are listed in Table 7.5.1. As a high temperature is employed within the extruder to melt the polymer for shaping, heat duty calculations can be performed. The heat duty for the extrusion process can be approximated from Equations 7.5.1-3:

$$Q_1 = mC_p(T_{melt} - T_{feed}) \quad 7.5.1$$

$$Q_2 = Heat\ of\ Fusion \quad 7.5.2$$

$$Q_3 = mC_p(T_{max} - T_{melt}) \quad 7.5.3$$

There will be two temperature changes in the extruder: one to bring the material from 25°C to 180°C (melting point) and the other from 180°C to 370°C, as the maximum possible temperature the material will reach based on friction and force within the extruder unit. As the PHB product is also melting, the heat of fusion will also be accounted for in the total heat duty. With this, the total heat duty was estimated to be ~20.3 kW (Table 7.5.2).

Table 7.5.1 Extruder Specifications

Parameter	Value
Max Capacity (kg/hr)	11000
Operating Pressure (MPa)	6.90
Operating Temperature (°C)	370
Length (ft)	7
Width (in)	6
Height (ft)	7
Process Flow (kg/hr)	~870

Table 7.5.2 Extruder Heat Specifications

Parameter	Value
Max Temperature, T_{max} (°C)	370
Feed Temperature, T_{feed} (°C)	25
Melting Temperature, T_{melt} (°C)	180[1]
Specific Heat Capacity, C_p (J/g °C)	1.40
Heat of Fusion, ΔH_{fusion} (J/g)	83.7[2]
Total Heat Duty or Power, Q_{total}, (kW)	20.3

[1] Melting Point of PHB from Tanadchangsaeng & Yu, 2012
[2] Heat of Fusion of PHB from Penkhrue et al., 2020

7.6. Cooling Trough

After extruding the PHB into strands, the strands will be cooled using a cooling trough. The strands will pass through a bed of cooling water on supporting rollers to lower the temperature. Using a cooling trough ensures uniform tempering of the PHB strands. We chose the KW 600 cooling trough by MAAG Group because it has an operating width of 400 mm

which is wide enough to cool 67 3 mm diameter strands simultaneously (MAAG Group, n.d.-b). This cooling trough will be paired with the compatible PWA 20 process water unit by MAAG Group to recycle the cooling water (see Figure 7.6.1) (MAAG Group, n.d.-b).

Figure 7.6.1. KW 600 cooling trough (left) and PWA 20 process water unit (right)

7.7. Air Knife

Next, the strands will be dried with an air knife to remove any water from the cooling trough. This step is necessary because we are feeding the strands into a dry-cut strand pelletizer. Moisture on the strands will lead to premature wear of the pelletizer so it must be removed. To remove the moisture, the strands pass over a suction box where the water is removed via suction air (see Figure 7.7.1).

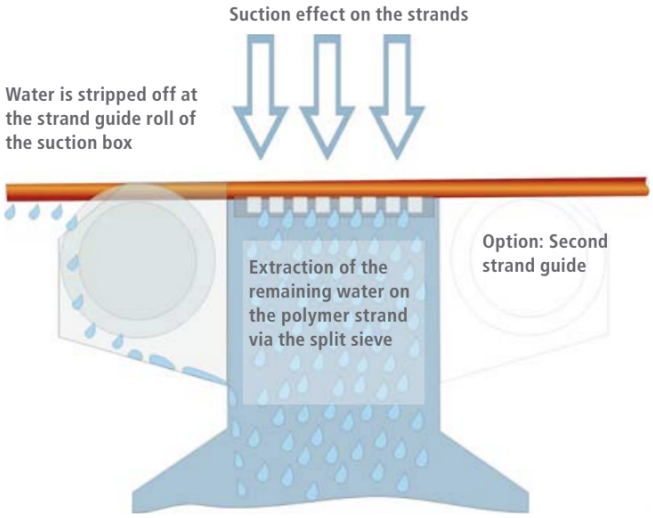

Figure 7.7.1. Air Knife Diagram

We chose the SE 400-2 Air Knife by MAAG Group because its working width allows the drying of 67 strands simultaneously (see Figure 7.7.2) . The motor and air flow rate is also sufficiently large enough to dry this number of strands (see Table 7.7.1). We considered using a compressed air powered air knife but decided against it because they are not as efficient as blower powered air knives (*Air Knife Blowers 101: How Do They Work?*, 2019) (MAAG Group, n.d.-d).

Figure 7.7.2 SE 400-2 Air Knife's Strand Guide and Split Sieve

Table 7.7.1. SE 400-2 Air Knife Technical Specifications

Specification	Value
Working Width (mm)	400
Number of strands	100
Suction Air Flow (m^3/min)	40
Blower Motor Power (kW)	7.5
De-watering	Pump

7.8. Pelletizer

Next, the dried strands are passed through a dry cut strand pelletizer to cut the strands into small 3mm length pellets. We chose the Primo 200 S by MAAG Group as our pelletizer because the cutting tools have a long service life (1000+ hours) and it utilizes a deposit free cutting head which should both reduce maintenance costs and downtime (MAAG Group, n.d.-c). This pelletizer can also process up to 1,350 kg PHB/hour by cutting 67 strands at a time which is approximately 40% greater than the expected PHB flow stream of 870 kg/hour through the pelletizer (see Table 7.8.1 and Appendix II).

Table 7.8.1. Primo 200 S Pelletizer Technical Specifications

Specification	Value
Maximum Throughput (kg/hr)	1,350
Process Flow (kg/hr)	870
Operating Width (mm)	200
Motor Power (kW)	3-11
Line Speed (m/min)	30-70
Maximum Number of Strands	67

7.9. Final Pellet Drying

To remove any residual moisture, the cut pellets are next fed to a centrifugal dryer. First, pellets are fed into the top of the dryer and the agglomerate catcher removes large pellet clusters that may clog the dryer. These clusters can be recycled back into the extruder to reduce wasted PHB. At the bottom of the chamber any pooling water is drained off, this expected to be negligible because the incoming pellet stream is expected to only by 0.8% water. Then, the pellets are fed to the rotor section of the dryer where the "both speed of rotation and the design of the lifters inside the rotor cause the pellets to move between lifters and screens while being conveyed by centrifugal action up the dryer rotor in a helical path" (MAAG Group, n.d.-a). In the upper ⅔ of the drying chamber, where the counter currently fed air removes surface moisture off the pellets (see Figure 7.9.1) . The pellets are expected to leave the dryer at a residual moisture of 0.05%, creating a final end product that is 99.95% PHB (MAAG Group, n.d.-a).

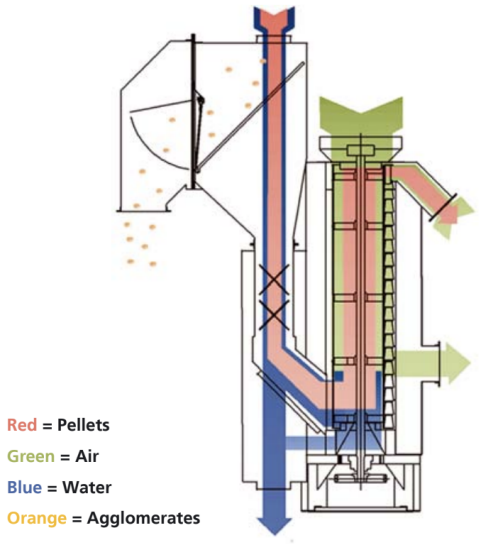

Figure 7.9.1 Centrifugal Dryer Diagram

We chose the EA 2008 Dryer by the MAAG Group because its operating capacity is slightly above our expected PHB stream of 870 kg/hour (see Table 7.9.1). It should be noted that this dryer can be used after either wet or dry cut strand pelletizers so its maximum water removal rate is far above the actual water removal rate.

Figure 7.9.2. EA 2008 Dryer

Table 7.9.1. EA 2008 Dryer Specifications

Specification	Value
Maximum Throughput (kg PHB/hr)	1,200
Process Flow (kg PHB /hr)	870
Maximum Water Rate (m^3/h)	20
Air Flow (m^3/h)	680
Motor Size (kW)	4

7.10. Pellet Packaging

Lastly, the dried pellets will be packaged into 25 kg bags of pellets. We expect to produce 7.320 kilotons per annum (ktpa) of PHB. This equates to packaging over 290,000 25 kg bags a year. To meet this specification we will need to package 35 bags per hour. We will use a manual

packaging system that can fill 60 bags per hour to do this. We intend to buy this system from Relco because they offer manual packaging systems of varying bag sizes and speeds (RELCO, n.d.).

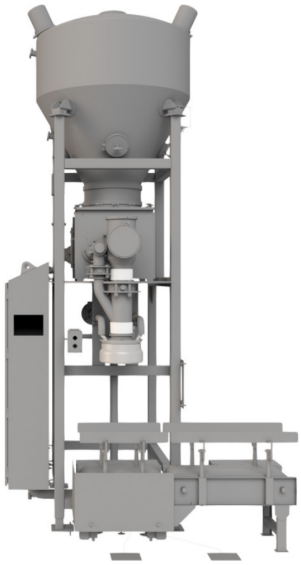

Figure 7.10.1 25 kg Manual Packaging System

7.11 Downstream Cleaning/Schedule

The homogenizers and centrifuges need to be cleaned periodically to prevent blockages or buildup of product in the pipes and valves. Similar to the upstream process, the downstream process also utilizes CIP systems that will flush the equipment with caustic solutions. In order to keep the process running continuously, extra equipment will be purchased so the equipment can be rotated as some units are being cleaned. Two extra primary centrifuges and one extra secondary centrifuge will be purchased, resulting in a total of 16 primary centrifuges and two secondary centrifuges.

8. Ancillary Equipment Design

8.1 Pump Design

Pumps are required to transfer material between unit operations. We first determined that pumps will not be used for material streams that are not very fluid or flowable or equipment that discharges material with force. For streams that are not flowable, the pressure differential was calculated using gravity head, actual pressure difference (if any), and frictional losses. There are three sources of frictional loss: piping, heat exchanger, or control valve loss. We allowed 0.5 atm each for piping, heat exchanger, and control valve losses. It is important to note that control valve losses are only accounted for when using centrifugal pumps. As a convention, centrifugal pumps were used when the volumetric flow rate was above 1 L/s, while under that threshold, peristaltic pumps would be used. Gravity head was accounted for when there was a significant vertical height difference between the inlet and outlet and this was calculated using Equation 8.1.1. The actual pressure difference is accounted for if there is a specific pressure difference between the inlet and outlet of the pump, such as a compressor pump. The total pressure differential is the sum of these three aforementioned components, in Pascals (Pa) (Equation 8.1.2).

$$Gravity\ Head\ =\ \rho g \Delta h \quad 8.1.1$$

$$(Gravity\ Head\ +\ Frictional\ Loss\ +\ Actual\ P\ Difference)\ *\ 101625\ Pa/atm\ =\ Pressure\ Differential \quad 8.1.2$$

A table of all of the pumps in the process, including differential pressures, flow rates, and hydraulic power requirements is located in Appendix III.

8.2 Storage Tanks

A two cycle (16 day) supply of the raw materials for the upstream process will be kept onsite in storage tanks, specifically crude glycerol, ammonia, acid, and base. The site will also have storage capacity for 30 days worth of production of the final packaged PHB.

Table 8.2.1 Storage Tank Volumes

Tank ID	Tank Contents	Volume (m^3)
T-101	Crude Glycerol	1250
T-102	Ammonia Hydroxide	170
T-103	Acid	2500
T-104	Base	300
T-105	Packaged PHB	510

9. Safety, Health, and Environmental Considerations

The main environmental considerations for this plant are the biological waste streams throughout the process. *C. necator* DSM-545 is a cultured bacterial strain that forms PHB inclusion bodies under nitrogen depletion. This strain is not a genetically modified organism (GMO), and thus can be released to a local wastewater treatment plant (WWTP). Additionally, the microorganisms are classified as risk group 1, meaning they are unlikely to cause infectious disease in humans (Schoeller, 2018). Regardless, live microorganisms will not be released in substantial amounts because the cells are lysed during downstream processing.

The waste streams from the downstream separation processes contain cell debris, unrecovered PHB, and water. The media centrifuged from the product fermenters (R-102) is at a neutral pH, so it will not have to be pH adjusted before being disposed of. The unrecovered PHB is a biodegradable polymer that does not require industrial composting. A study investigating biodegradation of PHB in municipal sewage sludge found PHB powder to degrade almost

entirely within two weeks (Gutierrez-Wing et al., 2010). The concentration of PHB powder in the study was 1,000 mg/L, and the concentration from our plant is approximately 5,800 mg/L. Assuming our industrial waste stream is mixed with other streams in the WWTP, the PHB should degrade in a timely manner before environmental release. Finally, the cell debris in the waste stream is naturally derived, as mentioned previously. The debris is expected to biodegrade in a WWTP into organic components.

In addition to the waste streams, the plant follows inherently safe and eco-centered design principles. We are employing only mechanical separation methods, such as centrifugation and homogenization, in the downstream process, rather than chemical separation. Additional solvent added throughout downstream is water, and the drying gas used is air. For upstream, the amount of aqueous sulfuric acid, ammonia, and potassium hydroxide are limited to what is necessary for pH control. Other environmental considerations, aside from the aforementioned chemicals, include process heat and gas production. Heat is transferred through either steam or cooling water throughout the plant. However, we will not be directly releasing cooling water to the environment. Instead, a cooling tower is used to recycle the cooling water, the design of which is outside the scope of this project. Steam is mainly a safety concern for plant workers and equipment maintenance. Finally, the plant will produce approximately 7.3 ktpa of CO_2 from fermentation off-gasses. This does not include CO_2 released through energy consumption in powering the plant, although the plant's energy carbon footprint could be reduced by taking advantage of abundant wind energy in Iowa (Iowa Environmental Council, 2022).

10. Societal Impact

Currently, the state of plastic pollution poses a safety concern for the environment. Furthermore, waste from multiple industries, plastic or not, also contributes to overall

environmental integrity and cleanliness. Plastic waste, left in oceans or on land, takes hundreds of years to decompose, which poses harm on surrounding ecosystems. The production of PHB provides not only a sustainable alternative to this global plastic issue, but also a solution. Plastics are relied on heavily in a plethora of industries, so the use of biodegradable plastics will allow for industries to continue normal function, but with an environmentally conscious mindset. These biodegradable plastics can be disposed of anywhere and will degrade quickly in the presence of microorganisms, without posing harm on habitats. By reusing and repurposing a biodiesel waste stream, which would otherwise be disposed of in sewage systems, the latter issue of waste can be addressed. Essentially, the design of this process could contribute to improving the state of plastic pollution by implementing PHB in manufacturing biodegradable plastics across many applications. Furthermore, we hope that the motivation for this project and the process design brings awareness to the damaging nature of plastics and the strong need for plastic alternatives amongst the larger discussion of climate change. In addition, the development of this plant will provide many jobs with sufficient pay/compensation for people with a range of industry experience. Currently, being in the midst of a recession, the availability of jobs for this plant would be encouraging and beneficial to those who are unemployed and struggling to find job openings.

11. Final Design Walkthrough

First, the raw materials, crude glycerol, ammonium hydroxide, and sulfuric acid, are supplied to the seed train (R-101) and product fermenters (R-102). Water will be fed and sterilized in place, while air will be fed into the seed (R-101) and product fermenters (R-102) after being compressed and filtered. The high density inoculum will be grown in the seed fermenters (R-101) with continuous nitrogen supply and sent to the product fermenters (R-102).

Each seed fermenter (R-101) is 16 m^3 in volume with two vertically spaced Rushton impellers that produce enough *C. necator* cell density to inoculate two product fermenters and the next seed fermenter. Each 100 m^3 product fermenter (R-101) has four vertically spaced Rushton baffled impellers where *C. necator* cells are grown and PHB is accumulated under nitrogen limiting conditions. Then, this fermenter effluent, made of cells, PHB, and water, is sent to the downstream processing units to isolate and purify the PHB product. In the first downstream step, this fermenter effluent is sent to the high pressure homogenization step, where two pairs of two homogenizers in series (H-201 and H-202) will lyse the cells at an operating pressure of ~40 MPa, releasing the PHB into the surrounding solution. This homogenate is then sent to the centrifugation process, which consists of two centrifugation steps, which both have a 96% removal efficiency for water and cell debris, and an intermediate mixing step for resuspension of the solids with more water. The first step employs 14 disc stack centrifuges each with a throughput of 2900 L/h, while the second step employs 1 disc stack centrifuge with a throughput of 9700 L/h. In the first centrifugation step (C-201), most of the water and cell debris is removed and the PHB mixture is sent to a mixing tank (MT-201), where more water is fed in and the PHB is resuspended, prior to another centrifuge (C-202). This second centrifugation step expels the remaining cell debris and water. The wet PHB is sent to a spray drying unit (SD-301) where moisture is removed to produce PHB at a 99.2% purity. Then, to prepare the PHB powder for the pelletizer, the material will be passed through an extruder (E-301). Here, the PHB powder is melted at a temperature of 370°C and force is applied to move the material through the die and form 67 homogeneous polymer strands. For the final processing units, the product flow rate is ~870 kg/hr, so a single extruder unit with a 10700 kg/hr capacity will be purchased for use. These long strands are then fed through a cooling trough to cool the strand from the extruder's

high operating temperature. Next, the cooled strands are passed through an air knife to remove any water that accumulated due to the cooling trough. The strands are then fed to the 1035 kg/hr capacity pelletizer unit (PE-301), which cuts the strands into small 3 mm pellets for sale, and is followed by a final drying step to remove any residual moisture in the pellets. Finally, to meet the plant's production target of 7.320 ktpa of PHB, 290,000 25-kg bags a year will be packaged and sold.

12. Economics

12.1 Major and Ancillary Equipment Costs

First, we determined the major equipment costs other than pumps. We used the cost estimator found in Towler and Sinnot. To account for inflation, we multiplied the 2015 estimate by the 2022 price index of 800 and divided it by the 2015 price index of 550. When we could not use Towler and Sinnot, we used equipment resale website equipnet.com and matche.com's equipment estimator to price our equipment. Both of these resources are recommended by Towler and Sinnott.

Table 12.1.1 Major Equipment Costs

Category	Tag	Description	Size	Price Per Unit	Quantity	Total Cost
Reactors	R-101	Seed	16 m^3	$541,000	9	$4,870,000
	R-102	Bioreactor	100 m^3	$2,030,000	24	$48,800,000
Compressors	CM-101	Air Filtration Compressor	73.9 kW	$19,000	11	$209,000
	CM-201	Spray Dryer Compressor	248 kW	$45,000	1	$45,000
Misc.	S-101	Air Filter		$1,580	33	$52,100
Solids Handling	H-201/ H-202	Homogenizer		$180,000	4	$720,000
	C-201	Centrifuge	0.61 m	$595,000	16	$9,530,000
	C-202	Centrifuge	0.33 m	$417,000	2	$834,000
	MT-201	Mixing Tank	2640 gal	$209,000	1	$209,000
	SD-201	Spray Dryer	350 kg/h	$815,000	1	$815,000
	E-301	Extruder		$70,000	1	$70,000
	CT-301	Cooling Trough		$1,250	1	$1,250
	AK-301	Air Knife		$362	1	$362
	PE-301	Pelletizer	900 kg/h	$4,850	11	$53,400
	CD-301	Centrifugal Dryer	900 kg/h	$894	9	$8,040
	MP-301	Manual Packaging		$9,800	1	$9,800
Product and feedstock storage	T-101	Crude Glycerol	1250 m^3	$362,000	1	$362,000
	T-102	Ammonium Hydroxide	170 m^3	$96,200	1	$96,200
	T-103	Acid	2500 m^3	$583,000	1	$583,000
	T-104	Base	300 m^3	$139,000	1	$139,000
	T-105	Packaged PHB	510 m^3	$197,000	1	$197,000
Cells		*C. necator*		$100,000	1	$100,000
					Total Major Equipment Cost	$67,700,000

Pump pricing was determined using a correlation from Turton et al. (2018) which is given by Equation 12.1.1, where C_p^o is the purchased cost of equipment at ambient pressure with carbon steel construction in September 2001 (CEPCI = 397), A is the capacity or size parameter (shaft power in kW for pumps), and K_1, K_2, and K_3 are values provided by Turton et al. for each piece of equipment.

$$log_{10}C_p^o = K_1 + K_2 log_{10}(A) + K_3[log_{10}(A)]^2 \qquad 12.1.1$$

Pumps were assumed to have an efficiency of 70%, so the shaft power was computed by dividing the hydraulic power by 0.7. As the majority of the pumps in this process have a shaft power requirement less than 1 kW, which is the minimum shaft power that can be used for the correlation, 1 kW was used in the computation of the costs for those pumps.

Table 12.1.2 Pump Costs

Pump	**Pump Type**	**Shaft Power (W)**	**Cost per Unit (2023)**	**Quantity**	**Total Cost**
P-101	Peristaltic	2.14	$6,050	10	$60,500
P-102	Peristaltic	25.6	$6,050	25	$151,000
P-103	Peristaltic	37.1	$6,050	10	$60,500
P-104	Centrifugal	423	$4,940	25	$123,000
P-105	Peristaltic	107	$6,050	10	$60,500
P-106	Peristaltic	1.57	$6,050	10	$60,500
P-107	Peristaltic	4.00	$6,050	10	$60,500
P-108	Centrifugal	1880	$5,250	25	$131,000
P-109	Peristaltic	12.6	$6,050	25	$151,000
P-110	Peristaltic	19.6	$6,050	25	$151,000
P-111	Peristaltic	12.4	$6,050	25	$151,000
P-201	Centrifugal	376	$4,940	2	$9,860
P-202	Centrifugal	384	$4,940	2	$9,860
				Total Pump Costs	$1,180,000

The most expensive piece of equipment is the 100 m^3 bioreactors. They account for 78% of the total equipment cost. We recommend finding used bioreactors instead which would lower the cost significantly, however we could not receive a price estimate for used reactors.

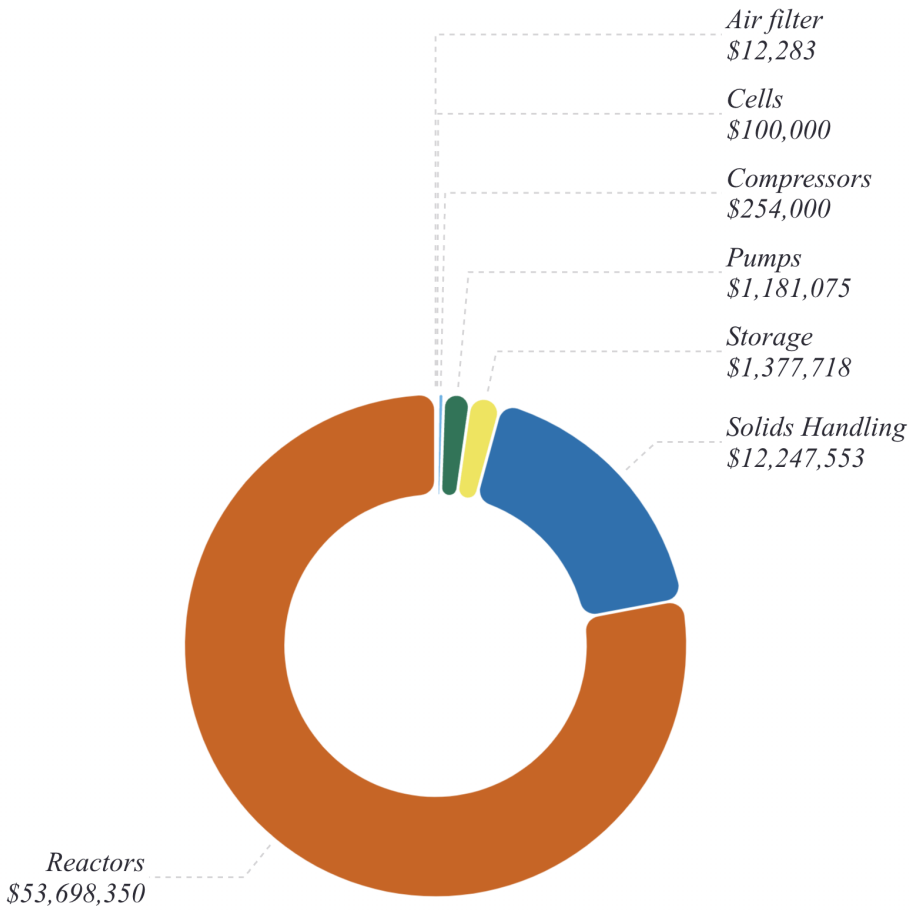

Figure 12.1.1 Equipment Cost by Category

12.2 Total Plant Capital Costs

The total capital investment of the plant is 461 million dollars. This includes the inside battery limits (ISBL) capital cost, offsite battery limits (OSBL) capital cost, engineering costs, and contingency cost. The ISBL investment is the cost of building the plant. This includes the cost of major equipment, bulk items such as piping, civil works such as roads, and installation

labor. To approximate the ISBL investment of this plant (C), the sum of the equipment costs ($\sum C_e$) was multiplied by a Lang Factor of 3.2 (see Equation 12.2.1). This is an updated Lang factor for the ISBL cost of 'Fluids-Solids' Process (Towler & Sinnott, 2012). Using this equation, the ISBL investment of the proposed plant is $229 million.

$$C = \sum C_e \times 3.2 \quad 12.2.1$$

The OSBL investment involves the cost of modifications made to the site infrastructure to accommodate a new plant. These modifications include electric substations, steam mains, cooling towers, laboratories, offices, and site security. As an initial estimate, Towler and Sinnott recommend the OSBL investment to be 40% of the ISBL, equating to $91 million (Towler & Sinnott, 2012).

The engineering costs involve the cost of contracting out detailed engineering design. Towler and Sinnot recommended the engineering costs to vary from 10-30% of the sum of the ISBL and OSBL costs. We took the average of this recommendation, 20%, and the engineering costs are estimated as $64 million.

The contingency charges are a buffer for any error in calculating the previous three estimates. Contingency charges account for changes such as minor changes in project scope and changes in price. Towler and Sinnot recommend accounting for contingency to be at least 10% of the sum of the ISBL and OSBL cost. We estimated the contingency to be $32 million.

Lastly, the working capital is the capital required to maintain plant operations. This includes: inventory feeds, spare parts, and cash on hand. The typical chemical plant has a working capital of 15% of the fixed capital; for this plant it would be $60 million.

Table 12.2.1 Summary of Capital Costs

Capital Costs	$MM
ISBL Capital Cost	220.5
OSBL Capital Cost	88.2
Engineering Costs	61.7
Contingency	30.9
Total Fixed Capital Cost	401.3
Working Capital	60.2
Total Capital Cost	461.5

12.3 Utility Costs

The plant requires utilities to operate. Steam is used to sterilize the bioreactors in place. Water is used throughout the plant such as for the bioreactors and resuspension. Cooling water is supplied to the jackets of the bioreactors to regulate temperature. Electricity is used to power the equipment and move cooling water throughout the plant. Compressed air is supplied to the fermenters and used to dry the wet PHB downstream. The annual cost of each utility was calculated using either approximations provided by Towler and Sinnot or by multiplying the electricity requirement by Iowa's industrial electricity rate (see Table 12.3.1). The most expensive utilities are process water ($4.1 MM/year) and equipment electricity ($3.8 MM/year). The total expense of the utilities is $9 MM/year.

Table 12.3.1 Summary of Annual Utility Costs

Utility	**Price**	**Annual Usage**	**Annual Cost ($/year)**
Steam	$0.5/ 1000 lb steam[1]	6.50×10^7 lb/yr	$32,477.38
Process Water	$3.07/ 100 ft^3 of water[1]	1.14×10^5 100 ft^3/yr	$4,187,734.76
Make-up Cooling Water	$0.02/ 1000 gal of water[1]	5.96×10^9 gal/yr	$119,228.75
Cooling Water Electricity	1.5 kWh/ 1000 gal of water[1]	5.96×10^9 gal/yr	$526,693.02
Equipment Electricity	$0.0589/kWh [2]	6.75×10^7 kWh/yr	$3,978,633.56
Compressed Air	$0.0589/kWh [2]	2.71×10^6 kWh/yr	$159,742.71
		Total Utilities Cost	$9,004,510.18

[1] Price estimates provided by Towler and Sinnot (2012)
[2] Iowa industrial electricity rate from Energy Information Administration (2023)

To calculate the total equipment electricity usage, the usage of each piece of equipment was calculated (see Table 12.3.2). For pumps, an assumed 70% efficiency was used. For all other equipment, we assumed 90% efficiency. The most expensive equipment to operate are the bioreactors (R-01 and R-02) and spray dryer compressor (CM-301).

Table 12.3.2 Equipment Annual Utility Usage

Tag	Quantity	Power (W)	Usage Per Year (Wh/year)	Annual Cost ($/year)
P-101	9	1.52	1.65E+05	$9.69
P-102	24	17.9	5.16E+06	$304.09
P-103	9	26.0	2.82E+06	$166.11
P-104	24	296	8.56E+07	$5,039.38
P-105	9	75.0	8.08E+06	$475.76
P-106	9	1.08	1.17E+05	$6.91
P-107	9	2.8	3.06E+05	$18.03
P-108	24	1320	3.80E+08	$22,394.76
P-109	24	8.80	2.54E+06	$149.79
P-110	24	13.7	3.96E+06	$233.16
P-111	24	8.68	2.51E+06	$147.73
P-201	1	263	3.17E+06	$186.57
P-202	1	269	3.23E+06	$190.46
R-01	9	20800	9.40E+08	$55,385.90
R-02	24	238000	2.78E+10	$1,637,342.00
CM-101	11	73900	3.97E+09	$233,622.82
CM-201	1	2480000	2.32E+10	$1,367,233.92
H-201/H-202	4	218000	8.16E+09	$480,737.09
C-201	14	5900	7.73E+08	$45,537.71
C-202	1	4500	4.21E+07	$2,480.87
MT-201	1	510	4.77E+06	$281.17
SD-201	1	45000	4.21E+08	$24,808.68
E-301	1	20300	1.90E+08	$11,191.47
AK-301	1	7500	7.02E+07	$4,134.78
PE-301	11	11000	1.13E+09	$66,707.78
CD-301	9	4000	3.37E+08	$19,846.94
			Total Equipment Electricity Cost	$3,978,633.56

12.4 Raw Materials Costs

The raw materials for this process are crude glycerol, potassium hydroxide, ammonium hydroxide, and sulfuric acid. In the table below, the price of each commodity is the 2022 market price published by either Argus Media (crude glycerol) or ChemAnalyst (all other raw materials). Although crude glycerol is a waste product of the biodiesel industry, the current market rate is $0.57/kg and it is our largest variable cost at $17 million/year.

Table 12.4.1 Raw Materials Costs

Raw Material	Price ($/kT)	Annual Usage (kT/year)	Annual Cost ($/year)
Crude Glycerol	569,712.18	29.900	17,034,394.18
Potassium Hydroxide (KOH)	1,329,000.00	1.774	2,357,082.50
Ammonium Hydroxide (NH_4OH)	1,115,000.00	3.494	3,895,783.24
Sulfuric Acid (H_2SO_4)	235,868.10	5.549	1,308,849.07
		Total Raw Materials Cost	$24,596,109.00

12.5 Fixed Costs

The fixed costs of the plant are labor, maintenance, and overhead expenses. The required operating labor was estimated using a correlation by Alkhayat and Gerrard found in Turton et al. (2018). The number of shift positions is given by Equation 13.5.1, where N_{OL} is the number of operators in each shift, P is the number of process steps dealing with particulate solids, and N_{np} is the number of nonparticulate processing steps.

$$N_{OL} = (6.29 + 31.7P^2 + 0.23N_{np}) \qquad 12.5.1$$

Using this equation, we determined the number of required shift positions to be around 30. For the total number of operators employed, this number is multiplied by a factor of 4.8 as recommended by Towler and Sinnott (2012) to correspond to a four-shift rotation with allowance

for weekends, holidays, and overtime. The operators each have a yearly salary of $50,000. We estimated that supervisors would be paid a salary of $150,000 and the plant would require five. Salary overhead, which includes employee benefits and training, was taken to be 40% of operational labor plus supervision costs (Towler & Sinnott, 2012).

Table 12.5.1 Labor Costs

Category	Number of Employees	Annual Cost ($/year)
Operational Labor	144	$7,200,000
Supervision and Management	5	$750,000
Direct Salary Overhead	--	$3,180,000
	Total Labor Costs	$11,130,000

Maintenance of the plant was approximated to be 3% of the ISBL investment, per Towler and Sinnot. We expect the maintenance to cost $12.04 MM/year. Overhead expenses cover plant overhead, tax, and insurance. Towler and Sinnot recommend the plant overhead be 65% of the combined labor and maintenance costs. This equates to $15.01 MM/year. The tax and insurance cost of the plant was approximated as 2% of the fixed investment as per Towler and Sinnot, or $6.02 MM/year (Towler & Sinnott, 2012). The total overhead of these two combined is $21.03 MM/yr (Table 12.5.2).

Table 12.5.2 Fixed Costs

Category	Annual Cost ($/year)
Labor	11,000,000
Maintenance	12,000,000
Overhead	21,000,000
Total Fixed Costs	44,100,000

12.6 Anticipated Revenue

Our anticipated revenue is based on the market price for PHB used for low-value consumption. As of 2010, PHB costs 4.50 US$/kg PHB (not adjusted for inflation) (Posada et al., 2011). This price aligns with current market values for PHA, which range between 2.40-5.50 US$/kg PHA (Crutchik et al., 2020). Compared with the lower price of 1.20 US$/kg synthetic plastic, there is already reduced demand for more expensive, bio-sourced plastics in single-use or low-value applications. Regardless, our plant intends to produce 7.32 ktpa of PHB and earn an annual revenue of $32,900,000. The manufacturing capacity of PHB worldwide is 27.2 ktpa, so we are increasing the current market by over 25% (Mostafa et al., 2020).

12.7 Return On Investment Analysis

Our return on investment (ROI) analysis yields a grim baseline economic scenario. Production and fixed costs far outweigh anticipated revenue for an average cash flow of -41.2 $MM/yr. The largest variable cost is raw materials at $24.6 MM/year. The largest fixed cost is the overhead expenses at $21 MM/year (Figure 12.7.1). Because we have a negative cash flow, this project will never turn a profit.

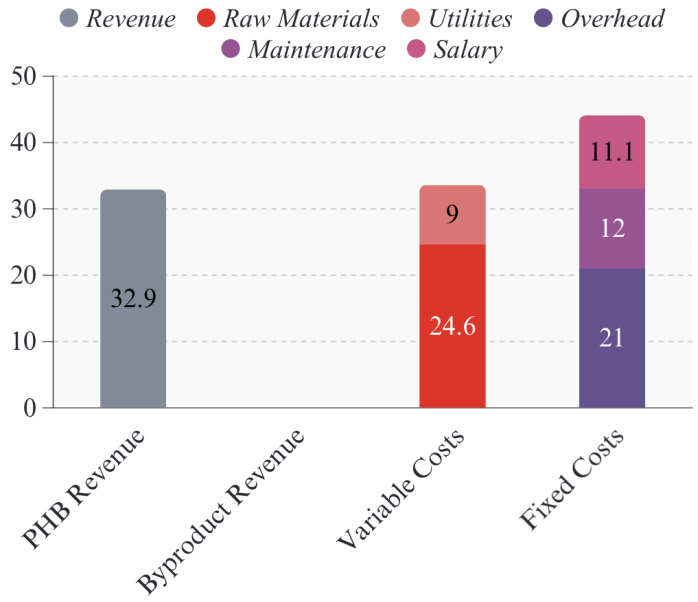

Figure 12.7.1 Revenue and Production Costs ($MM/yr)

In concert with plant capital costs, a discounted cash flow analysis of the plant was performed over the expected lifetime of the plant, 20 years, at a discount rate of 15%. As can be seen in Figure 12.7.2, the plant only loses money overtime and will never break even or turn a profit. It should be noted that depreciation for the ISBL and OSBL capital investment was accounted for with the straight line method over the first 7 years of plant operation.

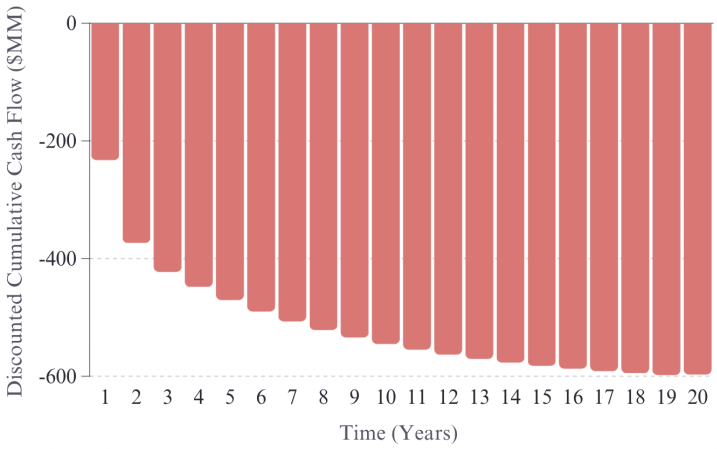

Figure 12.7.2 Discounted Cash Flow Analysis

12.8 Scenarios for Profitability

The baseline design of the process would never be economically feasible. We devised three scenarios to determine what action would be necessary to potentially generate profit. Our benchmark for a "successful" scenario was a 25% IRR after a 20-year plant lifespan. All of the proposed scenarios break even after 7 years.

Scenario 1: DOE Funding and Tax Credits for a Sustainable Process

The first assumption for this scenario is that we would partner with REG and receive our glycerol for free, reducing our raw materials cost by $17 million. As an offshoot of a renewable energy production process that transforms biodiesel waste into a usable product, the Department of Energy might also be interested in providing this plant with funding. For this scenario, we assumed we would receive funding from the DOE that would cover half of the total equipment costs. Finally, the US government gives tax credits to incentivize sustainable practices including use of renewable energy and production of sustainable materials. We determined that to achieve a 25% IRR at 20 years of operation, our plant would require $97 million in tax credits per year, indicating that this is an infeasible scenario.

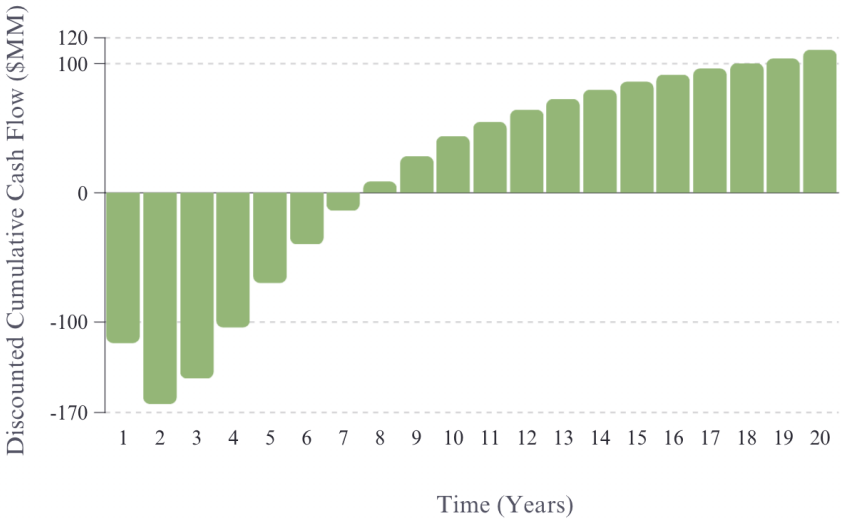

Figure 12.8.1 DCF Analysis of Scenario 1

Scenario 2: Scenario 1 with the Addition of New Bacteria with Higher Yield

On top of the conditions of Scenario 1, we considered the possibility of using a different microorganism with twice the productivity. That is, the biomass yield coefficient would be doubled from 0.34 to around 0.7 which indicates the maximum amount of PHB that could possibly be produced per amount of glycerol based on the carbon balance. *C. necator* was selected for its innate ability to produce PHB, but another microorganism such as *E. coli* could potentially be genetically modified to produce PHB at a higher rate. By assuming doubled yield, our product revenue would also be doubled. In this scenario, we would require around $64 million in tax credits. Realistically, we would also need to purchase more downstream equipment, so we would likely still require much more in tax credits.

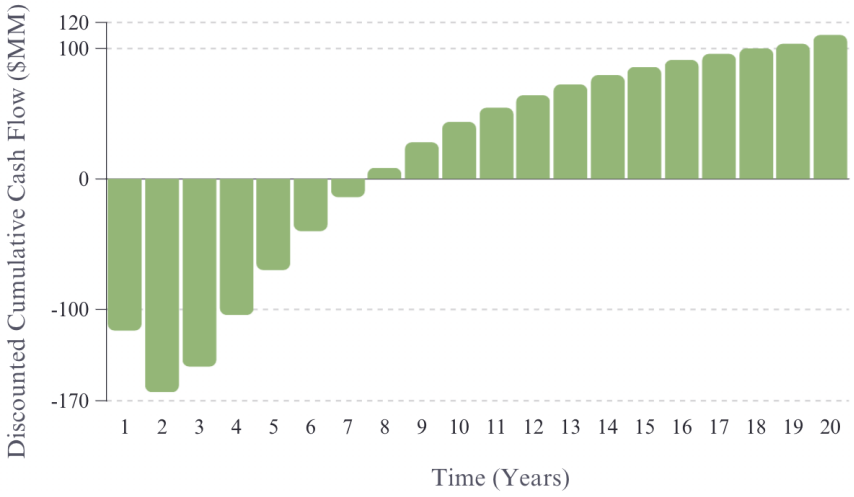

Figure 12.8.2 DCF Analysis of Scenario 2

Scenario 3: Selling to Biomedical Market

The biodegradable properties of PHB make it suitable for medical applications. Since demand for medical grade PHB is lower, we reduced the production scale to ⅓. We would buy glycerol from only one REG plant, rather than all three. Additional sterilization steps and further

purification would be required to sell the PHB as medical grade. To reach a 25% IRR, we would need to sell the PHB at a price of $27.80/kg.

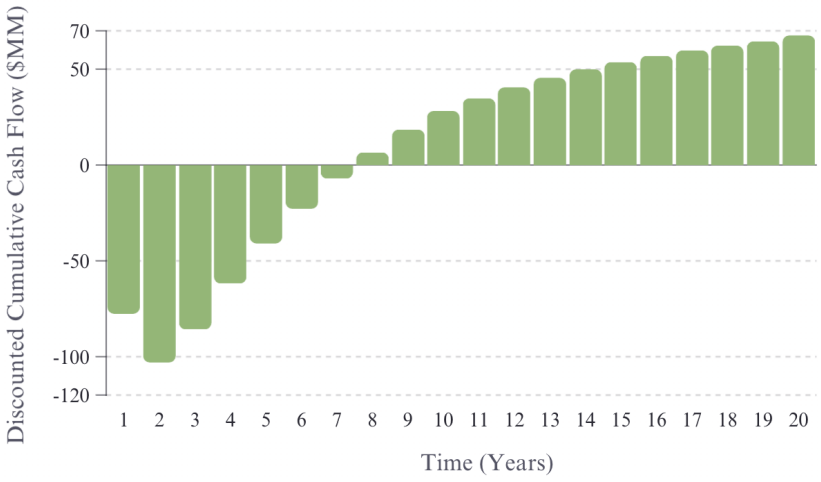

Figure 12.8.3 DCF Analysis of Scenario 3

13. Recommendations and Conclusions

13.1 Economic Feasibility

Given the design's economic reality and the scenarios for profitability, building this PHB plant is not economically feasible. While the concepts behind the plant are sustainable in theory, the design itself is not sustainable if it requires massive investments from federal funds or a dramatic change in market demand and value. In the 21st century, petrochemical-derived plastics are still far cheaper to produce and consume from a price standpoint. Until the human environmental health effects of plastic are included in this cost, it is likely a large-scale bioplastic plant will continue to be infeasible. However, there are future research avenues and project improvements to consider for entering the bioplastic market at a smaller scale.

13.2 Future Research & Project Improvements

Future research could explore a plethora of options. First, a different bacteria, with a higher productivity or growth rate, could be explored to increase the yield and decrease the upstream equipment demands of our plant. Furthermore, the production scope could shift to a different biodegradable plastic under the Polyhydroxy-alcanoates (PHAs) family. When holistically reviewing our process demands, we find that there is large water consumption, so future research could look into promoting higher yield with less water consumption or implementing an effective water recycle system in the process. In regards to the main raw material, crude glycerol, we assumed that trace amounts of fatty acid and ash in the crude glycerol would supply the microbes all of the micronutrients they need to grow. But, as an improvement, it would be beneficial to research the exact components that make up the impurities in crude glycerol to know whether the trace components are sufficient and beneficial or harmful for bacterial growth. Finally, this process could also be improved with the generation of more lab scale data surrounding aspects such as the growth kinetics of *C. necator*.

14. Acknowledgements

We would like to acknowledge our technical advisor Professor Eric Anderson for his guidance throughout the development of this design project. We would like to thank Professor George Prpich for his direction and support for the upstream design of this project as well as Professor Giorgio Carta for his insight regarding heat transfer mechanics and downstream process design. We would also like to thank Professor Ford for her insight into the seed train design.

References

Air Knife Blowers 101: How Do They Work? (2019, November 22). Atlantic Blowers. https://www.atlanticblowers.com/blog-post/air-knife-blowers-101-how-do-they-work/4

Cambiella, A., Benito, J. M., Pazos, C., & Coca, J. (2006). Centrifugal Separation Efficiency in the Treatment of Waste Emulsified Oils. *Chemical Engineering Research and Design*, *84*(1), 69–76. https://doi.org/10.1205/cherd.05130

Carta. (2022). *Bioseparations Lecture*.

Carta, G. (2021). *Heat and Mass Transfer For Chemical Engineers: Principles and Applications*. McGraw Hill.

Castillo, T., Flores, C., Segura, D., Espín, G., Sanguino, J., Cabrera, E., Barreto, J., Díaz-Barrera, A., & Peña, C. (2017). Production of polyhydroxybutyrate (PHB) of high and ultra-high molecular weight by Azotobacter vinelandii in batch and fed-batch cultures. *Journal of Chemical Technology & Biotechnology*, *92*(7), 1809–1816. https://doi.org/10.1002/JCTB.5182

Cavalheiro, J. M. B. T., de Almeida, M. C. M. D., Grandfils, C., & da Fonseca, M. M. R. (2009). Poly(3-hydroxybutyrate) production by Cupriavidus necator using waste glycerol. *Process Biochemistry*, *44*(5), 509–515. https://doi.org/10.1016/j.procbio.2009.01.008

Cressman, E. N. K., Tseng, H.-J., Talaie, R., & Henderson, B. M. (2010). A new heat source for thermochemical ablation based on redox chemistry: Initial studies using permanganate. *International Journal of Hyperthermia*, *26*(4), 327–337. https://doi.org/10.3109/02656731003614516

Crutchik, D., Franchi, O., Caminos, L., Jeison, D., Belmonte, M., Pedrouso, A., Val del Rio, A., Mosquera-Corral, A., & Campos, J. L. (2020). Polyhydroxyalkanoates (PHAs) Production: A Feasible Economic Option for the Treatment of Sewage Sludge in Municipal Wastewater Treatment Plants? *Water*, *12*(4), Article 4. https://doi.org/10.3390/w12041118

Dutt Tripathi, A., Raj Joshi, T., & Khade, S. (2019). *Preparative Biochemistry and Biotechnology Effect of nutritional supplements on bio-plastics (PHB) production utilizing sugar refinery waste with potential application in food pack*. https://doi.org/10.1080/10826068.2019.1591982

Ek, P., & Ganjyal, G. M. (2020). Chapter 1—Basics of extrusion processing. In G. M. Ganjyal (Ed.), *Extrusion Cooking* (pp. 1–28). Woodhead Publishing. https://doi.org/10.1016/B978-0-12-815360-4.00001-8

Global Filter. (n.d.). *BRPTFE-Series Bio-Burden Reduction Grade PTFE*.

Green, D. (2018). *Perry's Chemical Engineer's Handbook* (9th ed.).

Ghatnekar, M. S., Pai, J. S., & Ganesh, M. (2002). Production and recovery of poly-3-hydroxybutyrate from *Methylobacterium* sp V49. *Journal of Chemical Technology & Biotechnology*, *77*(4), 444–448. https://doi.org/10.1002/jctb.570

Gutierrez-Wing, M. T., Stevens, B. E., Theegala, C. S., Negulescu, I. I., & Rusch, K. A. (2010). Anaerobic biodegradation of polyhydroxybutyrate in municipal sewage sludge. *Journal of Environmental Engineering*, *136*(7), 709–718.

Harrison, S. T. L. (1991). Bacterial cell disruption: A key unit operation in the recovery of intracellular products. *Biotechnology Advances*, *9*(2), 217–240. https://doi.org/10.1016/0734-9750(91)90005-G

Iowa Environmental Council. (2022). *Wind energy*. https://www.iaenvironment.org/our-work/clean-energy/wind-energy

Jacquel, N., Lo, C.-W., Wei, Y.-H., Wu, H.-S., & Wang, S. S. (2008). Isolation and purification of bacterial poly(3-hydroxyalkanoates). *Biochemical Engineering Journal*, *1*(39), 15–27. https://doi.org/10.1016/j.bej.2007.11.029

Koch, M., Doello, S., Gutekunst, K., & Forchhammer, K. (2019). PHB is Produced from Glycogen Turn-over during Nitrogen Starvation in Synechocystis sp. PCC 6803. *International Journal of Molecular Sciences*, *20*(8), 1942. https://doi.org/10.3390/ijms20081942

Koch, M., & Forchhammer, K. (2021). Polyhydroxybutyrate: A Useful Product of Chlorotic Cyanobacteria. *Microbial Physiology*, *31*(2), 67–77. https://doi.org/10.1159/000515617

Kohn, M. (2019, July 15). *Finding New Life for Single-Use Biopharma Plastic Waste*. https://www.triplepundit.com/story/2019/finding-new-life-single-use-biopharma-plastic-waste/84231

Learn About Renewable Energy Group. (n.d.). Retrieved November 7, 2022, from https://www.regi.com/about

Li, Z., Yang, J., & Loh, X. J. (2016). Polyhydroxyalkanoates: Opening doors for a sustainable future. *NPG Asia Materials 2016 8:4*, *8*(4), e265–e265. https://doi.org/10.1038/am.2016.48

MAAG Group. (n.d.-a). *Centrifugal Dryer Pellet Processing Systems for the Plastics Industry*.

MAAG Group. (n.d.-b). *KW Uniform Cooling of Polymer Strands*.

MAAG Group. (n.d.-c). *Primo S Strand Pelletizing System for Best Pellet Quality*.

MAAG Group. (n.d.-d). *SE Strand Drying Prior to Cutting*.

Marks, D. M. (2003). Equipment design considerations for large scale cell culture. *Cytotechnology*, *42*(1), 21–33. https://doi.org/10.1023/A:1026103405618

McAdam, B., Fournet, M. B., McDonald, P., & Mojicevic, M. (2020). Production of Polyhydroxybutyrate (PHB) and Factors Impacting Its Chemical and Mechanical Characteristics. *Polymers*, *12*(12), 1–20. https://doi.org/10.3390/POLYM12122908

McNulty, C. (2016). Cleaning Bioreactors and Fermenters with CIP Systems. *Pharmaceutical Technology*, *40*(7), 46–48.

Meyer, H.-P., & Minas, W. (2017). *Industrial Scale Fermentation*. Retrieved February 16, 2023, from https://drive.google.com/file/d/107COWwJ8HwuJG7Z0-ez4fbXzf6NKwaPk/view?usp=drive_web&usp=embed_facebook

Mostafa, Y. S., Alrumman, S. A., Alamri, S. A., Otaif, K. A., Mostafa, M. S., & Alfaify, A. M. (2020). *Bioplastic (poly-3-hydroxybutyrate) production by the marine bacterium Pseudodonghicola xiamenensis through date syrup valorization and structural assessment of the biopolymer*. https://doi.org/10.1038/s41598-020-65858-5

Osmonics Inc. (1996). *The Filtration Spectrum*.

Penkhrue, W., Jendrossek, D., Khanongnuch, C., Pathom-Aree, W., Aizawa, T., Behrens, R. L., & Lumyong, S. (2020). Response surface method for polyhydroxybutyrate (PHB) bioplastic accumulation in Bacillus drentensis BP17 using pineapple peel. *PloS One*, *15*(3), e0230443. https://doi.org/10.1371/journal.pone.0230443

Polyhydroxybutyrate. (n.d.). Retrieved March 3, 2023, from https://polymerdatabase.com/polymers/poly3-hydroxybutyrate.html

Posada, J. A., Naranjo, J. M., López, J. A., Higuita, J. C., & Cardona, C. A. (2011). Design and analysis of poly-3-hydroxybutyrate production processes from crude glycerol. *Process Biochemistry*, *46*(1), 310–317. https://doi.org/10.1016/J.PROCBIO.2010.09.003

REG Glycerin Fact Sheet. (n.d.). Retrieved November 7, 2022, from https://www.regi.com/filesimages/fact%20sheet/reg-18114_glycerin_fact_sheet_update.pdf

RELCO. (n.d.). *25 Kg Manual Packaging System*.

Ritchie, H., & Roser, M. (2018). Plastic Pollution. *Our World in Data*. https://ourworldindata.org/plastic-pollution

Rotary Atomizer | Komline-Sanderson. (n.d.). Retrieved February 27, 2023, from https://www.komline.com/products/rotary-atomizer/#1550506157556-1f342dae-2851bb14-dce5

Rushton, J. H., Costich, E. W., & Everett, H. J. (1950). Power Characteristics of Mixing Impellers. *Chemical Engineering Progress*, *46*, 467–476.

Schoeller, A. E. (2018). *Technical Rules for Biological Agents (TRBA)* (5th ed., Vol. 53). Arbeitsmedizin Sozialmedizin Umweltmedizin. https://www.baua.de/EN/Service/Legislative-texts-and-technical-rules/Rules/TRBA/TRBA.html

Shuler, & Kargi. (2002). *Bioprocess Engineering: Basic Concepts* (2nd ed.).

Sims, B. (2011, October 25). *Clearing the Way for Byproduct Quality | BiodieselMagazine.com*. https://biodieselmagazine.com/articles/8137/clearing-the-way-for-byproduct-quality

SPX FLOW. (2017a). *APV Rannie 185Q / 275Q - Gaulin 185Q / 275Q Series | SPX FLOW*. https://www.spxflow.com/apv/products/rannie-185q-275q-gaulin-185q-275q-series-high-pressure-homogenizers/)

SPX FLOW. (2017b). *Anhydro Evaporation and Drying Solutions for the Chemical Industry*.

Tamer, I., & Moo-Young, M. (1998). Optimization of poly(β-hydroxybutyric acid) recovery from Alcaligenes latus: Combined mechanical and chemical treatments. *Bioprocess and Biosystems Engineering*, *19*, 459–468. https://doi.org/10.1007/PL00009030

Tanadchangsaeng, N., & Yu, J. (2012). Microbial synthesis of polyhydroxybutyrate from glycerol: Gluconeogenesis, molecular weight and material properties of biopolyester. *Biotechnology and Bioengineering*, *109*(11), 2808–2818. https://doi.org/10.1002/bit.24546

The plastic alternative the world needs. (2022, May 19). Klean Industries. https://kleanindustries.com/resources/environmental-industry-market-analysis-research/the-plastic-alternative-the-world-needs/

Towler, G., & Sinnott, R. (2012). *Chemical Engineering Design: Principles, Practice and Economics of Plant and Process Design*. Elsevier Science & Technology. http://ebookcentral.proquest.com/lib/uva/detail.action?docID=858659

Tullo, A. (2015). *The Final Hour For Biobased Plastics Maker Metabolix*. *93*(21).

US Biodiesel Plants. (2022). *Biodiesel Magazine*. https://biodieselmagazine.com/plants/listplants/USA/page:1/sort:state/direction:asc

US EPA, O. (2017, September 12). *Plastics: Material-Specific Data* [Collections and Lists]. https://www.epa.gov/facts-and-figures-about-materials-waste-and-recycling/plastics-material-specific-data

Vadlja, D., Koller, M., Novak, M., Braunegg, G., & Horvat, P. (2016). Footprint area analysis of binary imaged Cupriavidus necator cells to study PHB production at balanced, transient, and limited growth conditions in a cascade process. *Applied Microbiology and Biotechnology*, *100*(23), 10065–10080. https://doi.org/10.1007/s00253-016-7844-6

Waldrop, M. M. (2021). Bioplastics offer carbon-cutting advantages but are no panacea. *Proceedings of the National Academy of Sciences*, *118*(12), e2103183118. https://doi.org/10.1073/pnas.2103183118

Appendix

I. **Upstream Stream Table**

II. **Downstream Stream Table**

III. **Pump Table**